Ice-dominated Arctic deltas

Irina Overeem[1,2]✉, *Jaap H. Nienhuis*[3] *and Anastasia Piliouras*[4]

Abstract | Arctic deltas form the critical interface between the Arctic landscape and the ocean. They filter freshwater, sediment, carbon and biochemical fluxes from approximately 14 million km² of northern permafrost terrain. This Review highlights the unique controlling factors, seasonality and morphodynamic processes affecting Arctic deltas. Arctic deltas are 'ice-dominated systems' that are affected by land ice, permafrost and sea ice. They are strongly seasonal and are frozen for 7–9 months of the year. Permafrost limits channel migration. Arctic deltas experience ice jam floods, inducing biochemical exchange with thermokarst lakes. Transport under sea ice creates shallow prodelta ramps. Open-ocean conditions that promote marine reworking of river deposits are short-lived in the Arctic. A data compilation of Arctic deltas highlights that sediment and carbon fluxes are substantially lower than for lower-latitude deltas, with the exception of Greenlandic deltas. Arctic delta morphodynamics are also markedly subdued, with land–water conversion about eightfold less than in low-latitude deltas, probably owing to the unique ice processes occurring in Arctic deltas, which result in preferential floodplain and submarine sedimentation. Future trajectories of controlling factors indicate that Arctic deltas will transition away from being dominated by ice. The open-water season is expanding most rapidly, with wave energy predicted to increase threefold by 2100. Arctic deltas will thaw and experience increased wave influence, with poorly understood consequences for delta morphodynamics and carbon cycling. Process studies under transitional conditions are needed to develop predictive models further.

Delta
Depositional feature that forms where a river enters a standing body of water and supplies sediments more rapidly than they can be redistributed by wave and tidal processes.

[1]*INSTAAR, University of Colorado at Boulder, Boulder, CO, USA.*

[2]*Department of Geological Sciences, University of Colorado at Boulder, Boulder, CO, USA.*

[3]*Department of Physical Geography, Utrecht University, Utrecht, Netherlands.*

[4]*Earth and Environmental Sciences Division, Los Alamos National Laboratory, Los Alamos, NM, USA.*

✉*e-mail: irina.overeem@colorado.edu*

https://doi.org/10.1038/s43017-022-00268-x

Arctic deltas form where northern rivers enter the ocean and deposit sediments, building networks of distributary channels, often with extensive tundra flats strewn with thermokarst lakes (also known as thaw lakes). Arctic deltas house important ecosystems that support local communities[1]. Prehistoric people were not drawn to the Arctic deltas for settlement, unlike deltas in lower latitudes[2,3], but instead spread along the Arctic coast because of their reliance on marine resources. Only a few Arctic deltas are affected by humans, through upstream dams[4–6] or by mining of hydrocarbons, minerals and sand[7], making them some of the most pristine of all of the world's deltas[8,9].

Arctic deltas are integral components of the Earth's system. They form the critical interface between the Arctic terrestrial and ocean domains (FIG. 1). Approximately 16.5 million km² (11%) of the global landmass, and 13% of the global freshwater discharge drains to the Arctic coast, causing the surface of the nearly landlocked Arctic Ocean to be dominated by freshwater[10]. Arctic river drainage basins comprise most of the 13.9 million km² of Northern Hemisphere permafrost. These permafrost regions hold about 1,035 Pg of frozen carbon in their uppermost 3 m, which is approximately twice the pre-industrial atmospheric CO_2 content[11]. As rivers drain permafrost-affected basins, Arctic deltas are a filter for sediment, nutrients, carbon and heat to the Arctic Ocean[12–16] and are important modulators of the global climate and biogeochemical cycles[17] (FIG. 1; Supplementary Data).

Deltas are zones of river sediment deposition that act as efficient sinks of inorganic and organic material[18–20]. Arctic delta deposits store around 96 Pg of carbon[11,21,22]. With projected permafrost thaw looming, oxidation of soil organic carbon might trigger a feedback loop of carbon emission leading to climate warming and increased thaw. This permafrost carbon feedback mechanism is one reason why Arctic lowland deposits are a possible future hotspot in the global carbon cycle[11,23–27]. Biogenic methane emissions, another contributor to greenhouse effects, are also disproportionately high from Arctic lakes[28]. In addition, Arctic deltas store old, geological methane in their permafrost-capped subsurface, which might become a more substantial component of the world's methane budget as the permafrost thaws[29].

Because Arctic deltas are relatively understudied, fundamental questions remain about their morphodynamic processes. The quantity and timing of sediment, nutrient and heat exchange between fluvial systems and the marine environment are less certain than for other

Key points

- Arctic deltas are an important link in Arctic land–ocean exchange, delivering about 13% of the global freshwater flux but transferring a disproportionately low portion of the global sediment flux (around 2%) and particulate organic carbon flux (3–4%).
- River-ice jams during break-up cause substantial floods in Arctic delta plains, leading to pronounced sediment retention and biogeochemical flux exchange with thermokarst lakes.
- Land-fast sea ice plays an important part in river flood sediment distribution and acts to construct a characteristic submarine ramp, possibly enhancing carbon sequestration.
- Arctic deltas are currently ice-dominated and experience subdued morphodynamic activity compared with lower-latitude deltas, probably owing to slower channel migration and flow constriction from land-fast sea ice.
- Greenlandic deltas differ from other Arctic deltas in that they are growing rapidly owing to ice-sheet melt and their location in fjords protects them from wave action.
- Climate change will force a morphological adjustment of Arctic deltas that will include increased channel mobility, subsidence and increased coastal erosion caused by enhanced wave action.

deltaic systems[15,30]. The extent of sediment trapping and organic material sequestration that occurs in floodplains and in exchanges with the numerous thermokarst lakes is unknown[9,30]. Sequestration processes are closely interconnected with the strong seasonality of ice and its role in these systems[1]. River-ice jams cause flooding to be vastly different in Arctic deltas compared to temperate or ice-free deltas[31] (FIG. 2). The permafrost affects Arctic delta channel network morphodynamics: it strengthens banks and has long been thought to stabilize the river and delta channel network[32–36]. Sea ice affects river plumes and causes aggradation uncharacteristically far into the submarine prodelta[37,38]. The presence of sea ice also controls the duration over which waves can act as a morphodynamic agent.

A clearer understanding of Arctic delta processes is urgently needed in the context of rapid Arctic environmental change. Intensification of the hydrological cycle[39] and glacial melt[40] both affect water and sediment fluxes to the coast. Permafrost thaw slumps mobilize sediment and carbon and bring it into the river transport system[22,23,41]. Permafrost thaw may weaken the skeleton of the delta distributary channel network and promote more rapid geomorphic change[42]. Sea-ice coverage along the coast is decreasing[43,44], with potential impacts on wave-driven transport and delta shoreline erosion.

This Review discusses the unique controlling factors, seasonality, and morphodynamic processes affecting Arctic deltas (FIG. 2). We analyse deltas north of 60° N, representing most systems that contribute fluxes to the Arctic Ocean. We compile insights from classic field and laboratory process observations[33,36,45–56], previous reviews[1,7], and modelling and observational studies[37,38,57–59]. We use data compilations for the 6–8 largest deltas, which feature estimates of water, sediment and biogeochemical fluxes[12,13,15,16,30]. We expand our analysis to 387 Arctic deltas by including a model–data compilation that classifies over 10,000 global river outlets[60] (Supplementary Information). We contrast continental Arctic deltas with 75 deltas on Greenland[61,62] (BOX 1). This broad overview of Arctic deltas enables a better understanding of the unique controls and improved mapping of their future trajectories. Postulated trajectories are used to identify key knowledge gaps about changes in the transfer of freshwater, sediment and nutrients into the Arctic Ocean and the storage and release of carbon from Arctic deltas.

Long-term controls on Arctic deltas

The tectonic setting exerts a strong control on delta formation, with large deltas often located in subsiding basins[63]. The largest Arctic delta, the Lena Delta, is a prime example; it is aligned with the Gakkel Ridge, the ultraslow moving boundary between the Eurasian and North American plates[64,65]. Consequently, the Lena Delta is formed on slowly uplifting and subsiding tectonic blocks and its evolution and lobe switching during the Holocene are intricately associated with tectonic controls[54,66,67]. Similarly, the Mackenzie Delta is located in a zone of extensional fault basins associated with earlier rifting phases[68]. Much of the Arctic coast is tectonically quiescent[69].

Glacio-isostatic rebound is pertinent to Arctic deltas and drives crustal movements over timescales of 1,000–10,000 years. The Northern Hemisphere has been repeatedly occupied by large ice sheets over the Pleistocene. At the Late Glacial Maximum (21,000 years ago), continental ice sheets encompassed Baffin Island and Greenland as well as coastal mountain ranges, but left part of the Siberian and Alaskan near-coastal zones and shelves as ice-free refugia[70] with wide valleys draining towards the continental margin[69]. The enormous weight of ~3-km-thick ice masses caused the Earth's crust to deform downwards and the peripheral ice-free edges to bulge upwards. Since then, the ice sheets have melted, causing global sea level rise, and the removal of their weight led to an initially rapid elastic rebound of the continental crust in previously ice-covered regions. At present, a continuing reorganization of viscous mantle material flowing from the forebulges to former depressions contributes to uplift near past ice-sheet centres and to subsidence near former ice-sheet edges.

As a consequence, the sea levels under which Arctic deltas developed differ markedly from the global average (FIG. 3). The growth of most contemporary deltas globally initiated around 6,000 years ago, when post-glacial sea-level rise slowed along most of the Earth's coastlines[2]. Arctic delta evolution has been affected by the combined components of glacio-isostatic rebound and sea level history[1,46,54,66,71–73]. Many Arctic deltas near the centre of past ice sheets (that is, the Laurentide and Fennoscandian Ice Sheets) have experienced continuous uplift and relative sea level (RSL) fall after deglaciation[74,75]. Fjordhead deltas often have subaerially exposed depositional packages of marine sediments that are tens of metres thick[76,77]. The Geillini and Nastapoka deltas, which drain into the Hudson Bay (Canada), show a series of downstepping strandplains as a result of a RSL fall[78].

Arctic deltas further away from the continental ice sheets, such as the Severnaya Dvina delta in Russia[75], have experienced a mixture of uplift and subsidence. Most large Arctic deltas have undergone Holocene marine transgression, as on the Lena[66,71], Mackenzie[1,79] and Colville deltas[80]. Western Siberian bayhead deltas located in gulfs, notably the Ob, Taz, Pur, Yenisei and

Thermokarst lakes
Lakes occupying a closed depression formed by settlement of the ground following thawing of ice-rich permafrost or the melting of massive ice.

Permafrost
Ground (soil or rock, including ice and organic material) that remains at or below 0 °C for at least 2 consecutive years.

Glacio-isostatic rebound
The viscoelastic response of the crust that causes a rise of the Earth's crust after removal of the weight of large land-ice masses.

Forebulges
Flexural bulges in front of a load on the Earth's crust or upper mantle. The load, typically from ice or sediment, causes the lithosphere to flex by depressing the plate beneath it. The rate of forebulge formation and collapse is controlled by mantle viscosity.

Transgression
Movement of the ocean towards the shore, as a result of sea level rise.

Bayhead deltas
Deltas that develop at the innermost part of estuaries or bays within wave-dominated and mixed-energy systems on transgressive coastlines.

Khatanga deltas, which have upper delta plains of hundreds of km^2, experienced more rapid marine transgression after 5,000 years ago[69], and are currently prograding into their submerged, shallow palaeo-river valleys[66]. This transgression causes these systems to be located in estuaries and form bayhead deltas. Those Arctic delta systems located on the subsiding forebulge experienced faster rates of RSL rise compared to the global mean, even over the past 2,000 years[74,79,81–83] (FIG. 3).

Thus, sea level changes in the Arctic regions have been distinct over the Holocene and will remain distinct from global sea level change trends for centuries to come[84]. The effects on future sea level of the unloading of ice mass of the melting Greenland Ice Sheet will be superimposed[85] on the continuing gradual effects of rebound from the Pleistocene continental ice-sheet disappearance.

Modern controls on Arctic deltas

Rivers, tides and waves. Deltas worldwide are highly dynamic landforms that shape the land–ocean boundary. Delta morphologies are typically described in the context of relative river, tidal and wave-driven sediment fluxes[60,86–88], as well as sediment size[89] and cohesiveness[90,91]. River-dominated deltas are elongate and lobate, and form distributary channel networks through mouth-bar-induced bifurcations[88,92,93]. River-dominated deltas often propagate in shallow basins[92,94,95], and are prone to large-scale lobe switches[95]. Tidal deltas feature dense, dendritic networks of channels[86,96–98]. Tides widen, stabilize and maintain channels that are now disconnected from direct fluvial influx[99], and cause islands to have smoother boundaries[100]. Wave-dominated deltas are typically the most cuspate, with straight or gently curved sandy beach ridges. Depending on the obliqueness of incoming waves, the overall subaerial shape of wave-dominated deltas may be asymmetric[86,97,101–105]. To add to the complexity, many deltas are large enough that the proportion of controlling forces varies substantially along the coastline, which means that river sediment supply could dominate at the active river mouth, while waves and tides are dominant further along the delta front at abandoned lobes[97,98,106,107].

In general, wave, tidal and river sediment fluxes are lower in Arctic deltas than elsewhere around the globe.

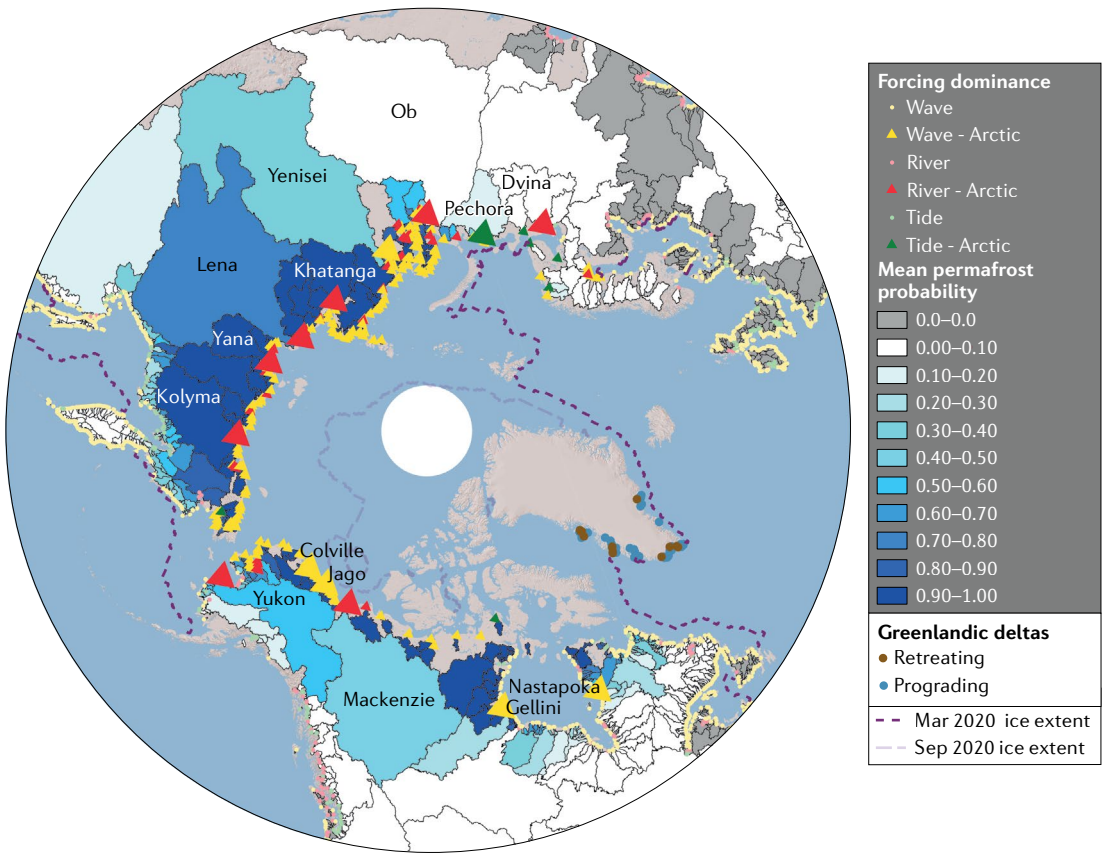

Fig. 1 | **Distribution and classification of Arctic deltas.** Circumarctic map of approximately 387 Arctic deltas and their contributing river drainage basins, as delineated from HydroSheds and ETOPO1 data[216,217]. On the basis of the dominant forcing factors, deltas are classified as fluvial-dominated, wave-dominated or tide-dominated systems[60]. River basins are shaded in blue by mean permafrost probability[17], which affects their incoming river sediment fluxes. All Arctic deltas are bounded by sea ice for part of the season, as shown by the seasonal maximum sea-ice extent for 2020 (dashed dark purple line), and experience open-water conditions in summer, as shown by the minimum sea-ice extent for 2020 (dashed light purple line). Greenlandic deltas are marked as retreating or prograding over the period 1980–2010 (REF.[61]). Deltas that are discussed in this Review are labelled.

Fetch
The distance that wind blows over open water and generates waves.

Observations of the sediment flux of the eight largest Siberian and North American Arctic river systems indicate a relatively low total flux of about 249 MT per year (about 2% of the global sediment budget)[12,30]. For comparison, the Mississippi River alone transports around 288 MT per year, and the Irrawaddy delta receives an estimated 259 MT per year[108]. Similarly, particulate organic carbon (POC) fluxes of Arctic rivers are estimated to be low, only 3–4% of the global flux[15]. Fluvial sediment fluxes to individual Arctic deltas range from relatively small for the respective basin areas in the Western Siberian region (for example, the Yenisei and Lena rivers) to higher on those rivers with more mountainous tributaries (for example, the Kolyma, Mackenzie and Yukon rivers; Supplementary Data). The POC fluxes for the Mackenzie and Yukon rivers are also higher than those of the Eurasian rivers[15]. Arctic river sediment data are sparse, and extrapolations have traditionally lacked data support for smaller river systems.

Tidal amplitudes and currents along the Arctic coast are small, with its main constituent below 0.3 m (REFS[7,109,110]). Exceptions to this general pattern are the White Sea deltas[111] and the Khatanga and Severnaya Dvina deltas in Russia, which are located in large estuaries with a tidal range exceeding 1 m (REFS[112,113]).

Although most Arctic deltas are exposed to the Arctic Ocean, wave heights are reduced because of sea-ice coverage that dampens waves and limits fetch. Potential further reductions in wave height near Arctic deltas stem from the relatively shallow continental shelf. The median shelf slope near Arctic deltas is 8×10^{-4}, compared with 3×10^{-3} for deltas globally[114].

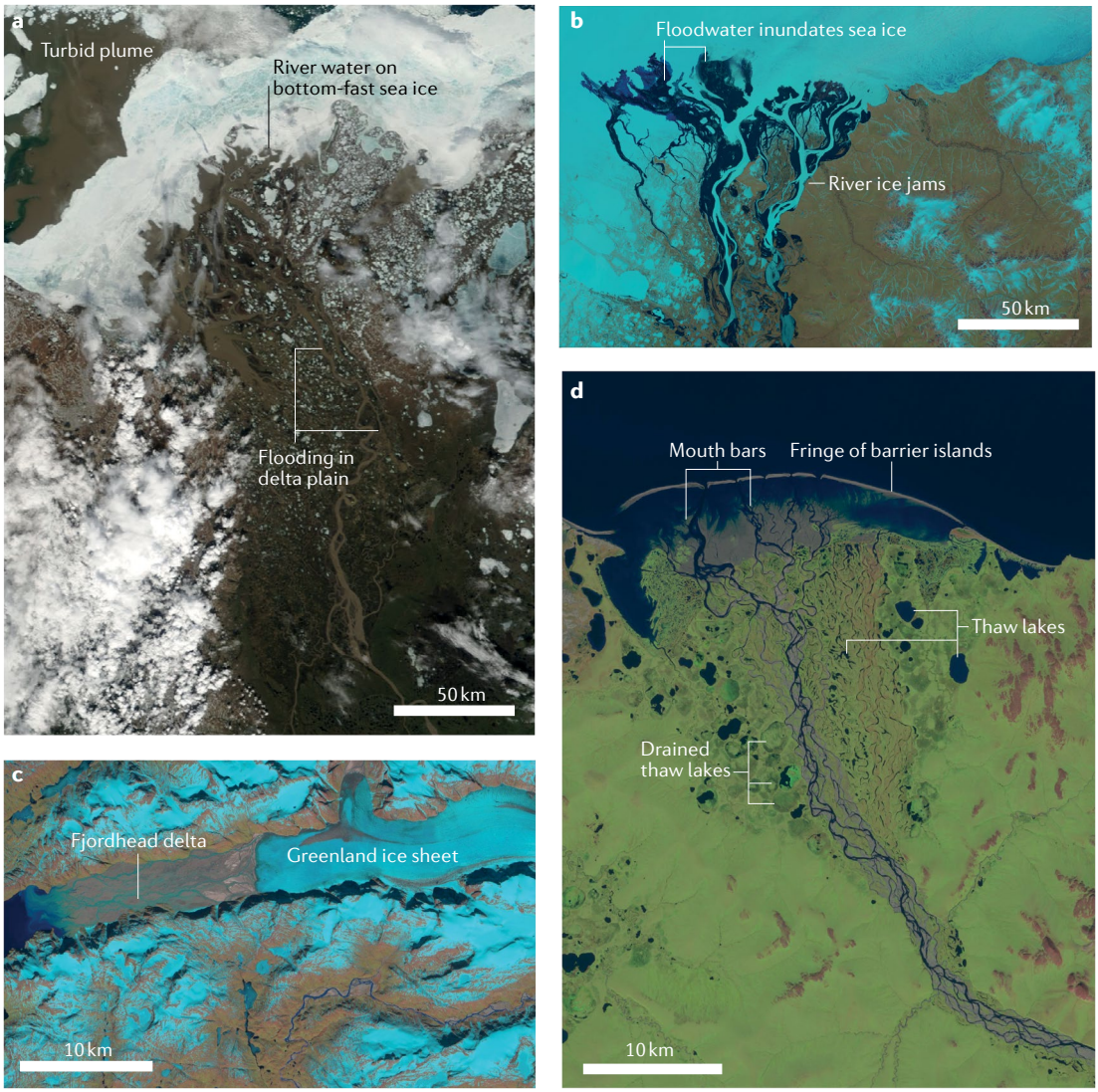

Fig. 2 | **Ice processes that act on Arctic deltas.** MODIS, Landsat and Sentinel satellite imagery illustrates the various ice processes that influence the morphodynamics of Arctic deltas. **a** | River-ice breakup and delta plain flooding and drainage of river water onto land-fast sea ice in the Mackenzie Delta, Canada (MODIS, 13 June 2001). **b** | Drainage of river water onto and below sea ice in the Kolyma Delta, Russia (Landsat 7, 30 May 2013). **c** | Glacial meltwater from the Greenland Ice sheet causes rapid river delta progradation in the Sermilik Delta, Greenland (Sentinel 2B, 23 May 2019). **d** | Wave erosion during the sea-ice-free open-water season shapes barrier islands and mouth bars near the delta front in Chukotka, Russia (Sentinel 2A, 25 August 2019).

Box 1 | **Greenlandic deltas**

Greenlandic deltas form unique end-members of Arctic deltas, and their morphodynamics are controlled by ice-sheet processes. Ice-sheet retreat and isostatic rebound control the late Holocene stratigraphic evolution of Greenlandic deltas[76,77]. Isostatic rebound amounted to tens of metres, so that many fjordhead deltas experienced a relative fall in sea level[76,225,226]. Usually, stair-stepped deltas formed, and subaerially exposed marine deposits mark previous sea level elevations (FIG. 3).

Modern Greenlandic deltas are river-dominated. Whereas Arctic deltas across North America and Siberia receive less sediment concentration than lower-latitude systems, the opposite pattern is true for Greenland, where approximately 1% of the global freshwater flux originating from ice-sheet melt delivers about 8% of the modern global suspended sediment[62,227]. High sediment loads are deposited by proglacial braided rivers, resulting in coarse-grained Gilbert-type deltas, which consist of a sandy delta plain (FIG. 2c), a steep submarine delta front and a finer-grained prodelta[76,227]. Proglacial lakes in the headwaters number in the thousands[228–230], but Greenlandic delta plains do not feature thaw lakes.

Many Greenlandic deltas are seasonally bound by sea ice[44]. In contrast to other Arctic deltas, sea-ice and river flood interactions do not have a profound role in the morphodynamics of Greenlandic deltas. Greenlandic deltas are mostly free of sea ice when river flow is high (associated with the warmest periods in summer, when extensive ice-sheet area contributes meltwater). In Greenlandic deltas in autumn, just as in other Arctic deltas, marine forces predominate for a short time, when river flow wanes. Wave-driven sediment transport can build sandy bars along delta fringes, but calculations for East Greenland deltas show that this wave-driven sediment transport is lower than fluvial sediment supply[224].

Coastline mapping of 75 Greenlandic deltas from the 1940s onward demonstrated that delta progradation has increased over the past few decades[61]. Of the 75 deltas with complete aerial photos and satellite records, only 47% had been advancing in the period 1940–1980. This proportion increased to 72% of deltas in the period 1980–2010 (FIG. 1). The mean progradation rate was mapped at 0.011 km^2 per year for these 75 Greenlandic deltas, with the most extreme delta progradation measured at 0.47 km^2 per year. Thus, for Greenland specifically, progradation indicates increased sediment delivery by ice-sheet meltwater[61]. It is unclear whether extreme sediment delivery from glacial lake outbursts[231–233] is a driving process of progradation, because statistical models indicate that increased river discharge alone suffices to explain delta growth[61]. In either case, Greenlandic delta systems are rare and are rapidly prograding, possibly sequestering carbon[20] and storing large amounts of sand resources[199].

Pronounced seasonality. Arctic deltas exhibit strong seasonality of river and wave processes. Major Arctic deltas convey 56% of their annual total water discharge in June, July and August, compared with 26% for lower-latitude deltas in the same period[115]. On the ocean side, sea ice limits wave and storm surge action on the coastal zone. Open water occurs only from late July to late October along much of the Arctic coast (Supplementary Data).

Arctic deltas are in a frozen, morphologically inactive state for most of the year. Snowmelt and runoff initiate south, in the headwaters of most drainage basins, typically in May. At that time, rivers and delta distributary channels are still covered in ice, and river-ice breakup occurs over several days with the arrival of spring runoff[116–119]. The ice thickness of water bodies, river channels and land-fast sea ice increases to 1.5–2.5 m over winter[118,120,121]. Depending on the year, as well as the river location and ice thickness, two mechanisms of river-ice breakup can occur: thermally (that is, weakened by melt of the ice itself), during a period of warm weather; or mechanically, by floodwater arrival and ice jamming[117].

For many Arctic deltas, peak river discharge coincides with or occurs shortly after river-ice breakup. The Colville, Lena and Jago deltas are examples of this concurrent river-ice break-up and arrival of the peak river runoff (FIG. 4). For some deltas, such as the Yukon Delta, peak runoff occurs weeks later (FIG. 4). Ice jams in the upper delta plain and bottom-fast ice in the shallower distributary channels create extensive flooding across the delta plain[35,122]. River flood waves spill over in thousands of thermokarst lakes, depositing sediments and delivering nutrients[4,24,123] (FIG. 2a).

Land-fast sea ice is still often present at the coast at the peak of river flow. River water can funnel its way underneath sea ice and can also drain onto the land-fast sea ice and cover it for short periods of time (FIG. 2c). This turbid standing water can extend out from the shore for tens of kilometres[124–126]. The energy and heat of river water can accelerate sea-ice break-up in Arctic deltas compared with that in nearby non-deltaic coasts[58,124,127,128].

Sea ice further away from Arctic deltas can linger into summer. Storm and wave action is subdued during this time owing to a limited fetch, resulting in decreased wave-driven sediment transport[43]. Warm summer conditions cause the active layer of deposits within the river basins and subaerial parts of the delta to deepen to its seasonal maximum thickness, and cause a short period of thaw slumping. High water temperatures increase the erosion of coastal permafrost bluffs[129,130] and potentially also frozen delta channel banks[35,131].

Air temperatures quickly drop in early autumn in the Arctic. The tundra starts to refreeze and the river water levels drop, resulting in limited fluvial activity. Storms are common during this period as the sea ice retreats to its yearly minimum. Wave energy is high and coastal flooding from storm surges can occur. Sea ice returns later in the autumn and results in a quick decline in wave action[132].

Ice processes. The presence of ice, both in river or delta channels and in permafrost deposits, affects erosional and depositional processes[1,7,57]. River ice, which is present during spring floods, influences sediment transport patterns and surface water transport (FIG. 5). River ice can lead to flow constriction underneath the ice and overbank flooding via increased backwater effects[37,59]. Under-ice flow constriction tends to increase flow velocities[133–135] and, from additional friction from the ice, maximum flow velocity occurs closer to the bed[135–138], thereby increasing shear velocities and sediment transport. There is a limit to this sediment-transport-enhancing effect. For smaller rivers, river ice can extend all the way to the bed with no flowing water during the winter. In that case, the frozen bed still needs to thaw out by spring melt water, and sediment transport is inhibited for the first weeks during spring floods[33].

Perhaps the most striking visible effect of ice processes on delta morphology is the abundance of thermokarst lakes. These lakes form by water ponding in topographic depressions, which thaws underlying permafrost, driving increased subsidence and further ponding[139,140]. Lakes cover up to 28% of the land surface on the major Arctic deltas[57] and are often connected to the channel network during the spring flood[59,141–143]. Some lakes may remain hydrologically connected for

Gilbert-type deltas
A type of fluvial-dominated delta forming a wedge of coarse sediments with parallel topsets and inclined foresets sloping downwards to the basin floor.

Land-fast sea ice
Ice that is anchored to the shore or ocean bottom, typically over shallow ocean shelves at continental margins. Fast ice is defined by the fact that it does not move with the winds or currents.

Thaw slumping
The process of slope mass movements caused by thawing of ice-rich permafrost.

Pack ice
Sea ice that is not attached to the shoreline and drifts in response to winds, currents and other forces.

much of the open-water season, and others near delta channels may be connected in the subsurface owing to thawed zones around the channel network[123] (FIG. 5d). Lake size is inversely correlated with mean annual temperature, so colder deltas feature larger lakes, presumably owing to a deeper permafrost that displays more continuous persistence[144]. Depending on flood patterns and duration, lakes may accommodate up to 50–70% of the spring flood volume on the Mackenzie Delta[59,145]. Lakes have been estimated to reduce suspended sediment loads to the coast by 18%, as fine sediments settle more readily in the slower-moving lake waters[1,59]. Overbank sedimentation rates observed in situ exceed 1 mm per year, but amount to 83 mm per year near channels[146]. It is estimated that the Lena Delta traps 70% of the incoming fine sediment load within the channel network before it reaches the ocean[54]. A study of 11 Arctic deltas in Russia estimates that 30–50% of fine sediment is trapped within the delta and postulates that 80–90% of bedload is deposited within the distributary network[113]. Given the longer residence times of sediment in lakes compared with in the delta channel network, lakes also have a large role in biogeochemical transport, increasing the POC and dissolved organic carbon (DOC) fluxes[1] and reducing nitrate and total phosphorus loads to the coast by 14%[147]. Thermokarst lakes therefore have an important role in Arctic delta hydrology, biogeochemistry and geomorphology[148].

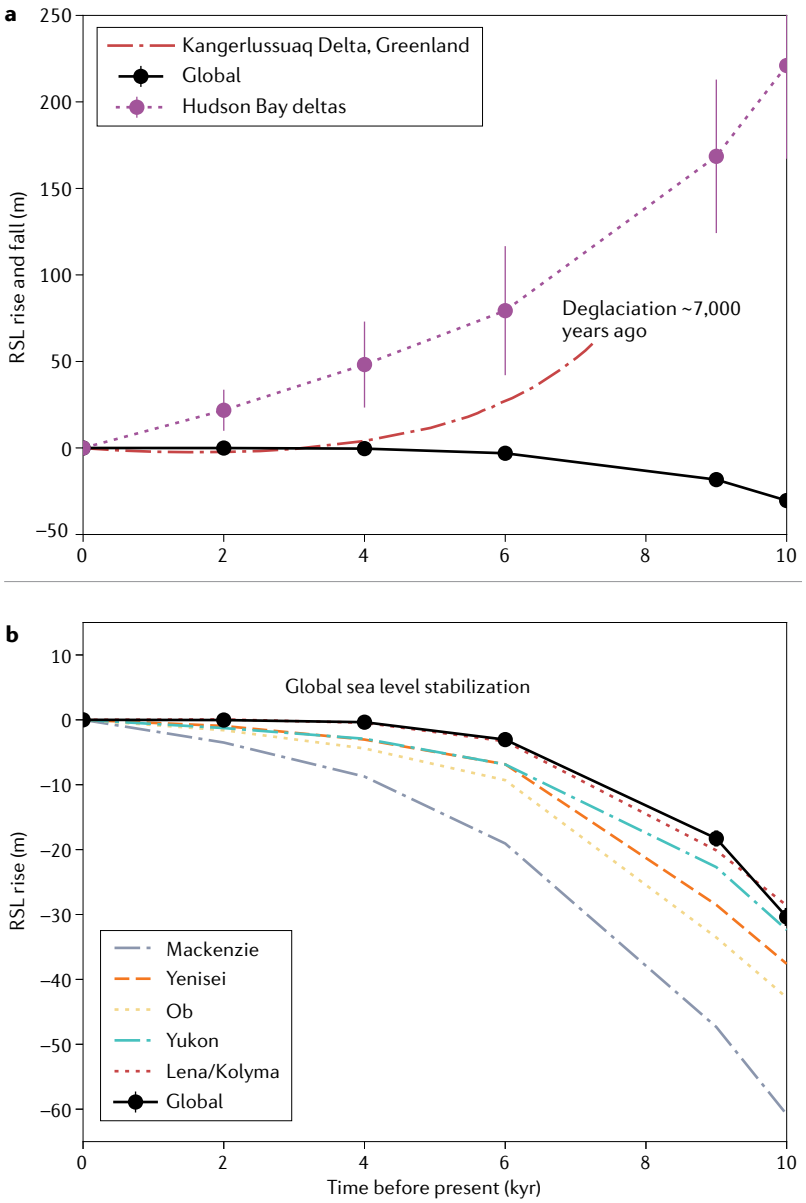

Fig. 3 | **RSL changes in Arctic deltas during the Holocene.** Graph of relative sea level (RSL) change during the Holocene for selected Arctic deltas and globally, as determined from the ICE-5G global glacio-isostatic model[67,78,80,84] and sedimentary reconstruction[71]. **a** | Deltas in the Hudson Bay region, Baffin Island and Greenland have undergone a fall in RSL over the early Holocene owing to rapid glacio-isostatic rebound of the land. Error bars represent standard deviations. **b** | Continental Arctic deltas have mixed sea level histories, with the Mackenzie, Yenisei and Ob deltas affected by forebulge effects after deglaciation, which has caused a continued sea level rise over the past 6,000 years once global sea level stabilized.

Beyond the floodplain, flow separation between under-ice and over-ice transport also occurs near the river mouth[125] (FIG. 5b). River floodwater spills over land-fast sea ice[56,58,124] and forms large areas of standing water, which only drains into cracks near the boundary of the land-fast ice and pack ice much further offshore. Under-ice funnelling of river floods and sediments can lead to enhanced sediment deposition in the near-shore zone. Laboratory experiments[38] and modelling of ice-covered deltas[37] showed that under-ice transport can lead to the development of a subaqueous ramp that can extend beyond the delta shoreline for tens of kilometres. Studies in the Yukon, Mackenzie, Yana and Lena deltas[53–56] showed that these ramps have sharp slopes at approximately the 2 m isobath, dipping to the inner shelf. Sediment suspended in the water column from late-season storms can be entrained during sea-ice refreezing by rising frazil ice, a process that occurs only in shallow water and may also contribute to the formation and maintenance of the flat ramp extending from the delta mouth bars[149,150]. Deposition of fine sediment and POC fluxes in these submarine prodeltas, as opposed to subaerial mouth bars, can promote more efficient carbon burial[151].

Permafrost, which underlies deltas bordering the Arctic Ocean, affects morphodynamics in several ways. Permafrost can reduce river channel migration rates[152] by delaying bank erosion because typically frozen soil must first be thawed before it can be mechanically eroded[34,153]. Long-term monitoring shows that the relative water discharge distribution between distributary channels in Russian Arctic deltas changes very slowly, at rates of 1–2% per decade[113], another indication of the relative stability of the delta distributary channel network.

Bank erosion is thought to occur in the summer months. River water temperatures can reach 15–16 °C in July[14,154] and can undercut ice-rich permafrost river channel banks to produce thermo-erosional niches[36]. Thermo-erosional niches trigger abrupt, large-scale bank collapse of the overhanging deposits. In repeat surveys, bank collapses may lead to apparently faster rates of bank migration over short timescales, such as local bank erosion rates reaching 30–40 m per year in the Mackenzie and Lena delta channels[54,155]. However, these rates are likely to be less representative of large

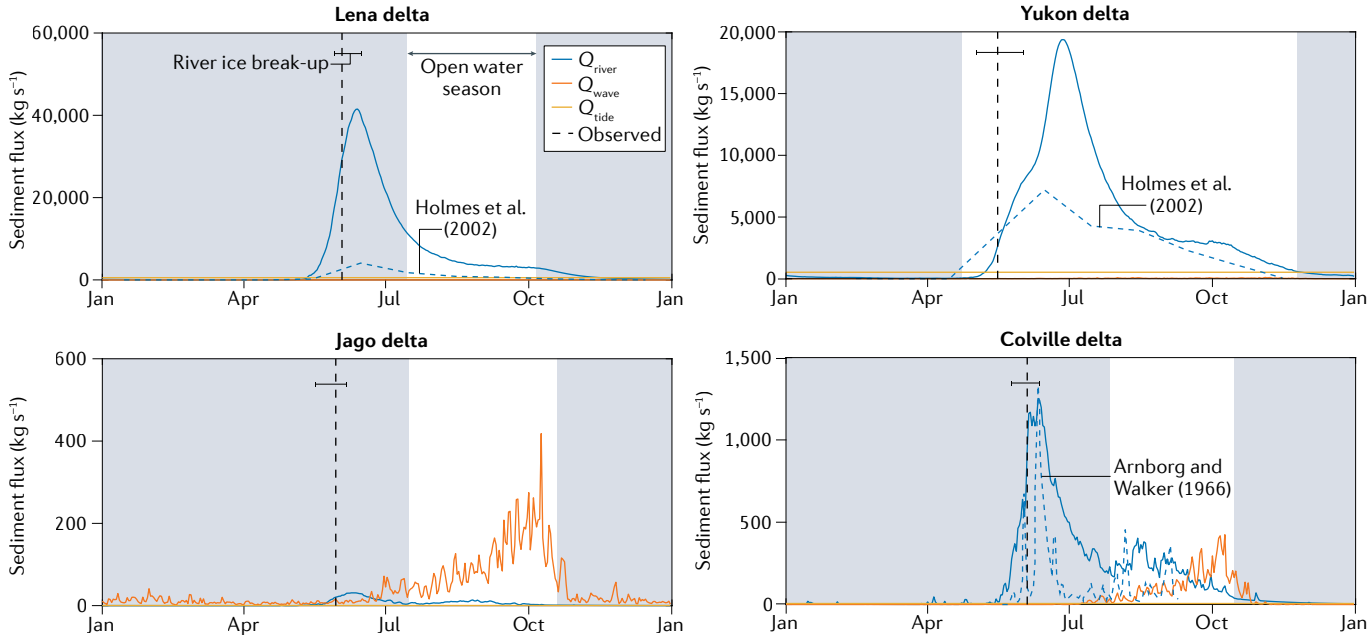

Fig. 4 | **Sediment transport processes in Arctic deltas.** The relative importance of modelled fluvial (Q_{river}), wave (Q_{wave}) and tidal (Q_{tide}) sediment transport processes in Arctic deltas over 1 year[60] are depicted in the graphs showing the mean daily sediment transport attributed to each process component for the period 1985–2015. We note that a typical year is likely to be flashier because of the temporal averaging. For those deltas for which observed river sediment transport data is available[30,49,218–220], these data are included (dashed blue line) for comparison. Dashed black lines mark the mean observed river-ice breakup days[115,221,222] (error bars indicate standard deviation). The mean measured presence of sea ice in the period 1985–2015 is indicated in light grey[43,44]. A comparison of the large fluvial-dominated delta systems, the Yukon Delta in Alaska and the Lena Delta in Russia, with the small river basin systems, the Jago and Colville deltas along the Beaufort Sea, reveals a distinct wave-dominated sediment transport season for deltas of smaller river systems.

stretches of channel and long time periods. Detailed measurements in the Colville River and delta document typical bank erosion rates of 1–3 m per year[36,152,156]. Most analyses of bank erosion rates are either based on annual repeat surveys or averages from multiple years of remote-sensing imagery and thus cannot conclusively mark the timing of highest bank migration activity. In studies of the Lena River, the fastest erosion is attributed to spring flooding, when the stage of the river can be several metres higher than during summer[36,54,155]. Interestingly, the temperature of the river water during spring flooding is still around the freezing point[14], which would inhibit efficient delivery of heat to the banks. In the Colville delta, channel banks consisting of peat are the most eroded[36]. Numerical modelling experiments corroborate that low erodibility of permafrost deposits in river deltas leads to a more stable channel network and fewer active channels than on deltas without permafrost[31,37].

Permafrost deposits are also exposed along abandoned sections of Arctic delta coastlines. Coasts along the Arctic Ocean recede at 0.5 m per year on average but many areas with high permafrost ice content display much higher rates of 15–20 m per year[157–161]. Small deltas along the Beaufort Sea coast retreated more slowly than the coastal average but were still erosive[162]. Exposed bluffs of the larger Mackenzie[107] and Lena[54,163] deltas also experienced rapid erosion of more than 10 m per year locally via thermal erosion from warm seawater, but coastal retreat rates for abandoned sections of Arctic deltas are generally more modest; for example, retreat averages 0.6 m per year for the inactive parts of the Mackenzie Delta coastline[107,164].

Frazil ice
Small needle-like ice crystals, typically a few millimetres in diameter, suspended in water, that represent the first stages of sea-ice growth. Frazil crystals merge under calm conditions to form thin sheets of ice on the surface.

Arctic deltas are ice-dominated

Ice strongly regulates two of the primary environmental controls of deltas: river and wave processes. Here, the unique characteristics and dynamics of Arctic deltas are summarized to show how existing classification schemes that consider only river, wave and tidal sediment fluxes do not fully account for the dominance of ice effects (FIG. 6).

Although several Arctic rivers have very high water discharges, conveying more than 10% of global river discharge, estimated sediment[12,30,108] and POC fluxes[15] from the large permafrost river basins to Arctic deltas are notably low. Modern fluvial sediment delivery to any delta apex from the permafrost landscape is roughly an order of magnitude lower than for temperate and tropical river basins of comparable size. In addition, Arctic river systems are active only for a short season. A coupled water balance and sediment flux model, WBMSed[165], shows that the ninetieth percentile discharge (representing the annual flood peak) is 60 times larger than the discharge of the tenth percentile (low flow conditions) in 387 Arctic deltas. For the median of over 10,000 deltas on the Earth, this ratio is 25, indicating that Arctic rivers are substantially flashier than the global average (FIG. 6).

Arriving at the river delta, these flashy but relatively low river sediment fluxes are then retained efficiently

Fig. 5 | **Ice processes in Arctic deltas. a** | River-ice break-up in Colville Delta (Alaska) showing ice floes on the Colville River (photo taken 21 May 2019). **b** | Example of a small delta along the Beaufort coast, Alaska, draining snow meltwater on top of fast-ice (photo taken 25 June 2008). **c** | Thermal river bank erosion in the distributary delta channel network of Canning Delta, Alaska (photo taken 25 August 2019). **d** | Connected and isolated thermokarst lakes in the floodplain of the Ikpikpuk Delta, Alaska (photo taken 12 August 2010). Photos in parts **a** and **c** provided by C. Arp and J. Koch, respectively.

in Arctic delta plains owing to ice jamming and associated flooding that routes sediments to the lake-rich delta plain[31].

Ocean waves have a limited season in which they can act on Arctic deltas, which results in delta morphologies that are distinct from those of temperate deltas. The median energy-weighted wave height for 387 Arctic deltas is 0.6 m, compared with 0.9 m for deltas globally, and the mean wave energy for Arctic deltas is 150 J m^{-2}, compared with 550 J m^{-2} for deltas globally[60,166]. These wave dynamics estimates for Arctic deltas are likely to be an overestimation, given that waves are modelled in deeper, open water rather than directly at delta shorelines, and estimates do not account for sheltering by barrier islands, lagoons or estuaries.

The third control, tidal processes, is less substantial in most of the Arctic Ocean than in oceans elsewhere, so that the effects of seasonal ice on river and wave processes becomes even more pronounced. The global delta data set[60] shows that the median tidal range for all Arctic deltas is only 0.2 m, compared with 1.2 m for deltas globally. Low tidal range, up to 0.2 m, is also modelled across the Arctic Ocean by a high-resolution tidal model (including data assimilations)[110]. Tide-dominated deltas in the Arctic are uncommon, despite low shelf slopes (FIG. 6a,h). The tidal range along the Arctic coast is simply too low to generate substantial tidal discharge. The OSU TPX tidal data set[109] is used here, a data set that has been well validated overall but might have insufficient coverage in narrower estuaries, so that some of the tidally affected Russian deltas are perhaps misclassified. In general, sediment aggradation on vegetated tidal flats, which is being increasingly recognized as an important stabilizing factor in Asian deltas, is of little consequence in Arctic deltas.

Many of the deltas with larger river sediment flux (for example, the Lena and Mackenzie deltas) are river-dominated[60] and contain many small-scale distributaries[167]. Low marine energy would typically increase progradation of foreset beds and prevent the establishment of large subaqueous clinoforms[168]. However, the presence of sea ice counters this effect and instead promotes the development of a large, shallow subaqueous ramp. This characteristic shallow prodelta was proposed as the identifying feature of ice-dominated deltas[48,52].

Some of these unique Arctic delta morphodynamics emerge from the analysis of satellite-derived water surface changes[60,169], and a quantitative comparison between Arctic and lower-latitude delta dynamics. Satellite mapping indicates that land–water conversion is nearly an order of magnitude less dynamic in Arctic deltas than in temperate deltas (FIG. 5c). The median land–water conversion for global deltas is 3×10^3 m^2 per year, compared with 0.5×10^3 m^2 per year for Arctic deltas. This difference is probably not only an effect of the aforementioned low sediment delivery. Accounting for the differences in fluvial sediment supply, land gain rates for Arctic deltas are 4.7×10^{-3} m^2 per m^3 of fluvial sediment delivered, compared with 17×10^{-3} m^2 of land per m^3 of fluvial sediment for global deltas (FIG. 6d).

Low delta land gain efficiency might be the result of high retention of sediment within the delta floodplain and lakes, a low preservation of sediment in the delta mouth bars and foresets, and flushing to the subaqueous bottomset.

To classify ice-dominated deltas, quantification of the forcing factors should include a sediment retention or floodplain aggradation coefficient that serves to limit fluvial sediment available to wave and tidal reworking at the delta front. With the inclusion of this retention coefficient, some deltas are expected to shift from a predicted fluvial-dominated regime to a possibly more realistic wave-dominated regime. Quantifying retention and efficacy of delta plain aggradation is also of importance for assessment of delta platform stability and drowning with respect to the delicate balance of sediment delivery, subsidence and sea-level rise.

In addition to river, wave and tidal sediment fluxes, Arctic deltas have also been affected by base level changes that are markedly different from those in temperate deltas. Over the long-term evolution of Arctic deltas, crustal movement caused by unloading of melting ice sheets has a profound influence on delta subsidence and sea level history. In general, continued glacio-isostasy is projected to lead to slower rates of sea level rise in the Arctic than in lower latitudes[74]. This a strong effect of land ice on Arctic deltas, although it operates over thousands of years.

Here, Arctic deltas are demonstrated to be uniquely dominated by ice, so that frequently used classification schemes cannot be applied without adaptations. Melt of the major ice sheets and isostatic rebound have affected the long-term evolution and current stability of Arctic deltas. Furthermore, permafrost landscape processes and ice-influenced sediment transport processes impact Arctic delta morphodynamics and sediment distribution between the onshore and offshore domains. In addition, ice strongly modulates fluvial and marine forcings. This ice dominance results in entirely unique deltas that, compared with lower-latitude deltas, are less morphodynamically active and have a different distribution of sediment between the floodplain, the subaerial delta front and the submarine prodelta. If a metric for ice-dominance were to be developed for Arctic deltas, it should include four key elements of these frozen environments: the presence of river ice during the spring flood, the overlap of the river flood arrival and the presence of land-fast sea ice, the abundance of permafrost, and the duration of the sea-ice-free open-water season.

Arctic deltas under a changing climate

The Arctic environment is already changing rapidly. For example, temperature has increased at more than twice the global rate[170] since 1970, matching expectations of Arctic amplification[171]. Warming impacts the terrestrial hydrological system by decreasing snow cover and by permafrost thaw[42,172–175]. River ice is thinning and break-up occurs earlier[118,119,143]. River-ice thinning affects winter travel and ice fishing and has been quantified in interviews with Yup'ik community

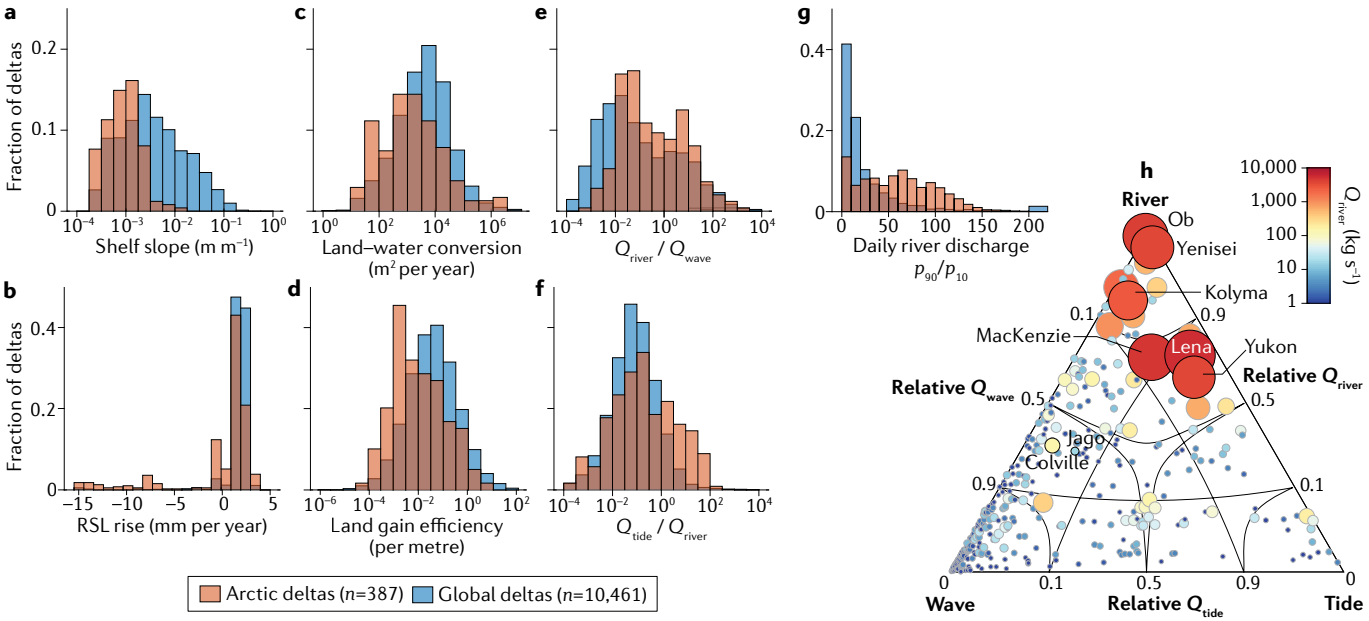

Fig. 6 | **Comparison of the characteristics and dynamics of Arctic and global deltas.** Graphs depict data for Arctic deltas ($n = 387$) and global deltas ($n = 10,461$). **a** | Arctic deltas form on lower shelf slopes[223], resulting in a lower morphodynamic contribution of wave forces. **b** | Many Arctic deltas experience relative sea level (RSL) fall or anomalously low RSL rise compared with deltas globally (records are for 1985–2015)[224]. **c** | Arctic deltaic coastal zones show less land–water conversion than for global deltas, as determined from Landsat records for 1985–2015. **d** | Shown as a ratio of modelled sediment delivery, Arctic deltas gain less land than global deltas. **e** | The ratio of modelled river sediment transport to wave sediment transport is higher for Arctic deltas than for global deltas. **f** | The ratio of modelled tidal sediment transport to river sediment transport is more variable for Arctic deltas than for global deltas. **g** | River discharge is flashier for Arctic deltas than for global deltas, indicated by the 90th percentile divided by the 10th percentile of daily discharge values for 1980–2010. **h** | Modelled relative importance of key sediment transport processes for Arctic delta systems demonstrates that the deltas of the six largest river basins (Ob, Yenisei, Kolyma, Mackenzie, Lena, Yukon) are clearly fluvial-dominated systems, many smaller deltas are wave-dominated systems, and very few Arctic deltas are tidally dominated systems.

members in the Yukon–Kuskokwim delta[176]. River discharge increased by 7–10% over the past 30 years or more and the timing of peak floods has shifted to earlier in the spring[115,173,177,178]. Glacier and ice-sheet melt has accelerated from the 2000s onwards[179,180]. Consequently, fluvial inputs to deltas are expected to increase.

However, change in the Arctic Ocean is even more pronounced than on land. Seasonal sea ice coverage rapidly decreased over the past 40 years. Passive microwave satellite data shows that the sea ice minimum extent for 15 September 2020 was only 3.74×10^6 km^2, 40% lower than the average seasonal sea ice minimum over the reference time period of 1981–2010 (REF.[181]). At the coast, the median duration of the 2012 open-water season, in comparison to 1979, expanded by 1.5–3-fold for different Arctic coast sectors[44]. This expansion is asymmetric, with most of the lengthening occurring in October and early November. As a result, the longer open-water season and increased winds have caused higher significant wave heights throughout the Arctic Ocean, especially in autumn[182]. Regionally, these changes amount to about 20% higher late-season wave heights over the past 40 years[183]. Of note, these wave model analyses are coarse-resolution and not as applicable for shallow-water waves and nearshore conditions, or for deltas in sheltered bays. The prominent shallow 2 m subaqueous delta ramp stretching out over tens of kilometres, as is typical in many Arctic delta systems, may have a role in dampening wave impact.

The impact of these dramatic environmental changes over the past decades on coastline change in Arctic deltas has been investigated. Automated land area change detection over the Landsat record for 1985–2015 demonstrates that directly along the coastline, most Arctic deltas appear relatively stable, with a small mean net area increase of 0.5×10^3 m^2 per year. This relative stability is remarkable, considering that sediment fluxes to these deltas are pristine and fluvial delivery has been increasing. The fact that overall the deltaic coastline is rather stable or erosion dominates can be explained in several ways: retention and trapping of sediment in the delta plain is efficient in Arctic delta systems; progradation of the subaerial delta is comparatively modest, and a lot of sediment is transported to the subaqueous delta and shelf and thus remains invisible to remote-sensing mapping of land area changes; or wave energy delivery has increased faster than riverine influence and reworks progradational mouth bars, or erodes abandoned stretches of the delta shoreline more rapidly than background rates.

Most climate model simulations project the Arctic region to continue to become much warmer than present at the end of the twenty-first century[184]. Empirical work relates warming to future fluvial sediment fluxes. Every 2 °C of climate warming is projected to increase sediment flux by 22%[185]. The WBMSed model shows increases in sediment delivery of 7–9% for the Yukon and Lena deltas and a modest 3% reduction in sediment delivery to the Mackenzie Delta as a result of dam construction[186]. Comparison of observed and modelled fluvial fluxes for the past 30 years shows that there can be large discrepancies when predicting fluxes for any individual delta system (Supplementary Fig. 1). Moreover, these estimates do not account for changes in river ice or in sediment trapping in the upstream floodplain due to ice jam floods. Thus, any estimates of ungauged rivers and of future fluvial sediment fluxes for Arctic deltas are highly uncertain.

Future warming will continue to profoundly affect sea-ice conditions. By 2050, the Community Earth System Model forced by Representative Concentration Pathway 8.5, a high-emission scenario, projects that all Arctic deltas will experience two more months of open water each year[187]. Notably, the Yukon Delta is projected to be completely free of sea ice by 2100 (REF.[187]). The rapid expansion of the open-water period will dramatically increase wave energy. Modelled future wave climate[188] has been used to calculate wave-driven sediment transport for Arctic delta systems[60]. For deltas along exposed coastline stretches, wave-driven sediment transport could increase by 150–300% by the end of the twenty-first century in comparison with 1979–2009, while in the more sheltered areas the increases amount to 50–150% (Supplementary Fig. 2). Again, these analyses are uncertain, and sediment transport may be more dampened in the immediate delta front region. However, doubling or tripling of the energy delivery from marine processes far outpaces estimations of changes in fluvial sediment transport.

Geomorphologically, the warming and thawing of permafrost in Arctic deltas will likely increase rates of landscape change, including faster rates of bank erosion and channel migration that will threaten communities living on the banks of delta channels. Eroding ice-rich channel banks could become a more important source of previously frozen carbon into the river and delta channel network (FIG. 7).

Permafrost degradation is also expected to drive increased rates of subsidence due to the loss of ground ice that will lower the land surface[189,190], making deltas more vulnerable to sea level rise (FIG. 7). In the Yukon Delta, permafrost heaves the tidal flats by as much as 1 m in comparison to nearby areas of low ice content[191]. Because river ice currently enhances flooding that has been shown to increase rates of aggradation on the delta plain, the loss of river ice may decrease rates of flooding and aggradation, which, combined with permafrost thaw subsidence, will make Arctic delta plains highly susceptible to both long-term drowning and storm surge flood events if the projected increases in fluvial sediment loads cannot balance the rate of land surface lowering[146]. The loss of ice cover during spring floods may also diminish the role of the sub-ice channel network in transporting riverine sediments to the deeper ocean and the 2 m ramp (FIG. 7). Faster rates of subaerial Arctic delta progradation might therefore be expected in an ice-free or warmer Arctic, given that fewer sediments will be lost to overbank aggradation and offshore transport, such that they may instead contribute to shoreline growth. However, the rate of progradation is likely to be limited by the increased wave activity during the longer open-water season, which can redistribute sediments in the nearshore zone.

Historically, Arctic deltas have been dominated by sparse permafrost tundra vegetation[191,192]. Research

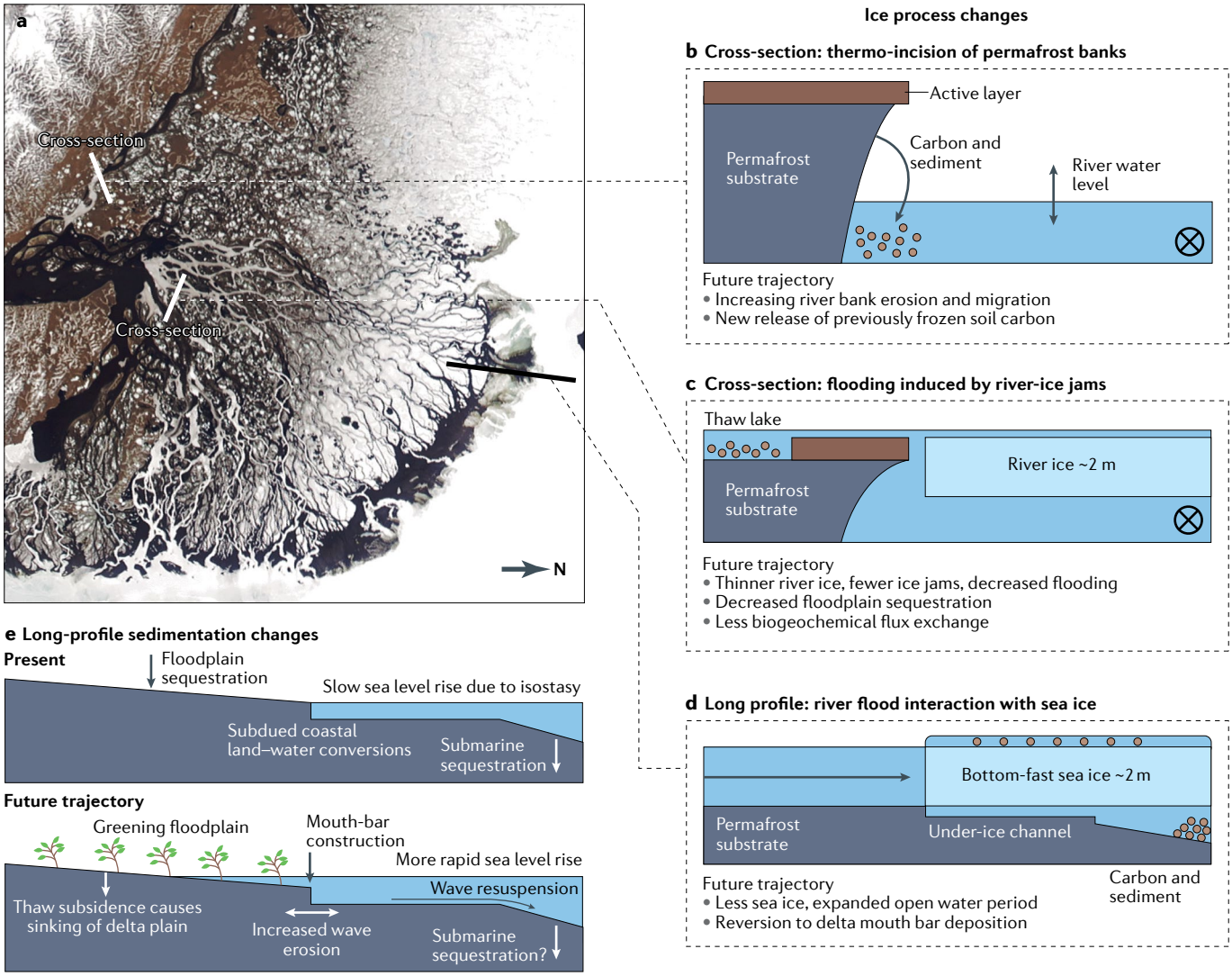

Fig. 7 | **Current concepts of Arctic delta processes and projected effects of climate warming.** NASA MODIS Aqua imagery of the Lena Delta (eastern Siberia, Russia), on 6 June 2019, showing the current ice-dominated delta environment (part **a**). Schematic cross-sections depicting current ice processes and projected changes for permafrost river banks (part **b**), channel–floodplain exchanges (part **c**) and along-channel interactions between the river flood water and the sea ice (part **d**). Present source-to-sink sediment distribution for Arctic deltas and projected changes with climate warming (part **e**).

suggests a greening of the Lena Delta between 1999 to 2014 that reflects increased aboveground biomass, possibly due to shrub expansion[193]. The greening is most prominent near the delta channels and is hypothesized to be the result not only of warmer air temperatures but also of wetter conditions near the active channels associated with permafrost degradation and/or flooding[193]. By contrast, in the Yukon–Kuskowin coastal delta, ecotypes have changed over the decades but the most important change was a loss of shrubs: birch and heather ecotypes declined in favour of sedge meadows and lowland marshes. Much of this ecotype change was attributable to a major storm surge flooding event and associated saltwater intrusion[191]. As shrubs expand[192], tundra vegetation height increases[194] and the greening continues across the Arctic, vegetation may play a more important part in trapping sediments on delta plains and in increasing bank strength (FIG. 7). Bank strength will decline as permafrost degrades, but if vegetation is able to establish quickly enough as channels mobilize and sediments thaw, then the denser or more extensive vegetation may provide a new stabilizing element to Arctic delta channel networks. More rapid establishment of vegetation on newly formed land, which is not an important process at present, would also mean that Arctic deltas could become more of a 'blue carbon' coastal system[195] in the future.

Summary and future perspectives

Arctic deltas are the filters of water, sediment and nutrient fluxes draining from the Northern Hemisphere permafrost terrain to the Arctic Ocean. As such, they are an essential element of the global Earth System and its hydrological and biogeochemical cycles. At present,

Arctic deltas are unique due to the influence of ice: permafrost, river ice and sea ice. Permafrost terrain has lower sediment yields, river ice induces early season flooding and results in floodplain sedimentation, and permafrost riverbanks migrate slowly. Sea ice blocks delta mouth-bar deposition and dampens wave action. These distinctive processes also affect how carbon is stored in different parts of an Arctic delta source-to-sink system; exactly how is a topic of active study.

Ice dominance seems to result in morphologically more stable delta systems in the Arctic than in lower latitudes. This relative stability is even more unexpected because it has persisted over the past few decades, despite rapid change in many of the controlling climate factors in the Arctic, indicating that there is latency in the response of delta systems to change. However, rapid change in all three elements of the cryosphere and the Arctic climate is projected to continue, most profoundly in the ocean domain. Consequently, Arctic deltas will probably become less dominated by ice and more dynamic. Arctic deltas will also experience considerably more wave-driven transport and become increasingly affected by storm surges. These changes will happen in an Arctic region that is opening up to international shipping[196,197] and will experience shifts in hydrocarbon[198] and other resource exploration[199] and both subsistence[200] and commercial fisheries[201]. This review demonstrates that there are still large unknowns in current and future delta dynamics. Predictions that include thermal controls on morphodynamic and biochemical processes present a grand challenge. We call for further field, modelling and laboratory studies of the transition of Arctic deltas.

Over the past decade, compilation of massive remote-sensing data sets and implementation of advanced processing techniques (for example, long-term records of passive microwave data for sea ice and Landsat imagery for vegetation and coastal morphological change) have revolutionized our ability to automate mapping of environmental and morphological change. An Arctic-wide high-resolution topography data set, ArcticDEM, similarly modernizes terrain analysis. At the same time, numerical models of the coupled Arctic atmosphere–cryosphere–ocean system have advanced and are valuable for quantifying and predicting regional climate, permafrost state[17], ice-sheet melt, sea-ice conditions[202,203] and wave climate[166,188]. Data sets of environmental controls, traditionally in the domain of climate modellers, can now be more easily probed by hydrologists, geomorphologists, ecologists, biogeochemists and sedimentary geologists. These data–model integrations should advance our understanding of the conditions of a vastly larger number of Arctic deltaic systems, and highlight the role of more Arctic deltas that are controlled by small rivers and wave-dominated conditions.

However, neither remote-sensing nor large-scale Earth system models can resolve more detailed surface processes and landscape change processes. There is a pressing need for field observations to augment remote-sensing data analysis and Earth system modelling. Long-term in situ monitoring of permafrost has not focused on deltaic sites, owing to their water-logged nature and potential for rapid disturbance by natural processes. Smaller Arctic rivers are neither gauged nor sampled, and data on long-term sea levels, tides and wave climate are sparser for the Arctic than for lower latitudes.

Here, we identify two priority areas in which field observations will be crucial to obtain a better understanding of the dynamics of Arctic deltas and their role in the global carbon cycle. First, quantifying sediment distribution across different subdomains within Arctic deltas is key to understanding their morphodynamics. Considering the extreme seasonality of Arctic deltas, field observations should focus on two understudied periods: river-ice break-up and the spring flood season, and the late open-water season. Field measurements of water and sediment transport and deposition during river-ice break-up and peak flood interactions with land-fast sea ice would inform our estimates of fluvial sediment distribution across different zones within delta systems. Measurements during the late-season storms would better inform how storm surges affect deltas[204] and how wave transport may change. These periods are short-lived and challenging for in situ observations but for many Arctic deltas a disproportionately large amount of the annual sediment flux occurs over short timescales and events. Innovative observation techniques, such as using sedimentation elevation tables and steel monuments to assess delta plain aggradation and ground subsidence, are already being pioneered in lower-latitude deltas and the Mackenzie system[146]. Better methods of assessing bedload transport would also be beneficial. Novel methods, such as drone-based observations, time-lapse cameras and autonomous sensors may allow for data collection of water temperatures, turbidity, river-ice and channel-network activity, flood water depths across the floodplain, and perhaps even characteristics of the coastal land-fast ice, such as thickness, late-season wave heights and storm surge flooding during times that are difficult to observe.

Second, urgent questions remain regarding carbon release, pathways and sequestration in Arctic deltaic systems. To better quantify the permafrost carbon feedback mechanism, we need an inventory of permafrost carbon content of riverbanks and measurements of carbon cycling along water transport pathways, as well as residence times of carbon within the transport corridor and deltaic channel network. Sampling and laboratory analysis of river water and floodplain and delta plain soils are key additions to existing databases[11,21]. Furthermore, sediment cores of submarine prodelta deposits can shed light on carbon sequestration in the offshore domain. A focus on representative, smaller delta systems may allow for more comprehensive in situ field campaigns across a deltaic floodplain and distributary network.

Once the current processes in Arctic deltas are better constrained with both metadata analysis and new field data, a grand challenge is to bring this knowledge into predictive frameworks. Numerical models are essential to make predictions of the future state of Arctic deltas. However, both the ice processes that make Arctic deltas unique as well as carbon dynamics are largely missing from current morphodynamics and sedimentary process

Excess ice
The volume of ice in the ground that exceeds the total pore volume that the ground would have under natural unfrozen conditions.

models. To predict Arctic delta evolution, we envision that coupled permafrost–morphodynamics models will be needed, but such coupled models require a number of advances.

Permafrost models of varying complexity[17,205–209] have been employed to investigate the future state of permafrost. Although air temperature remains a dominant control on permafrost behaviour, other boundary conditions, such as snow thickness, vegetation coverage and surface-water content, are problematic to resolve in detail at present. To best predict responses of deltas to sea level rise, it is essential that the ability to predict ground subsidence by tracking melt of excess ice is included in permafrost models.

Improved models should incorporate new theory for the mechanisms of sediment and carbon transport during river-ice break-up. Thermal channel bank erosion is another process to add to existing morphodynamics models, before contributions of bank erosion to total sediment and carbon fluxes can be resolved. Theory developed for the thermal erosion of coastal bluffs[129,130,210,211] and thermal bank erosion[34] in combination with river temperature models[154] already exists to develop these capabilities further in predictive models, but fundamentally new approaches to lateral erosion in morphodynamics models are required[212].

An additional important process is the interaction of river water with land-fast sea ice. An innovative model of plume behaviour on land-fast sea ice sufficiently captured the distribution of river water above and below the fast ice[58] but has not explored effects on morphological change. Incorporating process rules for interactions between river ice and sea ice influences the migration dynamics of a deltaic network and creates incised submarine channels and a subaqueous shallow ramp[37], typical of Arctic delta systems, but an opportunity exists to explore these and more complex process interactions in more robust physics and fluid dynamics models.

To add realism to wave reworking near deltas, ongoing improvements in modelling wave–ice interactions in the marginal ice zone[132,213–215] will improve on the wave models available at present. Importantly, refining current model predictions to better represent wave dynamics in the shallow nearshore zone will be a critical improvement compared to the current data, which are representative only of water depths exceeding 30 m. Improved capture of nearshore wave dynamics will aid in understanding of wave resuspension and the export of fine sediment and associated carbon to the offshore sink. Both theoretical improvements and higher-resolution coastal morphology change predictions are essential, given that we expect open-water conditions to expand dramatically, much more so than riverine influxes.

Published online 15 March 2022

1. Forbes, D. L. in *Coasts and Estuaries* Ch. 8 (eds Wolanski, E. et al.) 123–147 (Elsevier, 2019). **This is a comprehensive review of process studies in the Mackenzie Delta and Canadian fjord deltas.**
2. Stanley, D. J. & Warne, A. Holocene sea level change and early human utilization of deltas. *GSA Today* **7**, 1–7 (1995).
3. Mason, O. & Friesen, M. *Out of the Cold: Archeology on the Arctic Rim of North America* (The Society for American Archeology, 2018).
4. Bobrovitskaya, N. N., Zubkova, C. & Meade, R. H. Discharges and yields of suspended sediment in the Ob' and Yenisey Rivers of Siberia. *IAHS-AISH Publ.* **236**, 115–123 (1996).
5. Vörösmarty, C. J. et al. Anthropogenic sediment retention: major global impact from registered river impoundments. *Glob. Planet. Change* **39**, 169–190 (2003).
6. Lehner, B. et al. High-resolution mapping of the world's reservoirs and dams for sustainable river-flow management. *Front. Ecol. Environ.* **9**, 494–502 (2011).
7. Walker, H. J. Arctic deltas. *J. Coast. Res.* **14**, 718–738 (1998). **This classic paper reviews Arctic deltas with lessons learned from 30 years of field studies in the Colville River delta**.
8. Tessler, Z. et al. Profiling risk and sustainability in coastal deltas of the world. *Science* **349**, 638–643 (2013).
9. Syvitski, J. P. M. et al. Sinking deltas due to human activities. *Nat. Geosci.* **2**, 681–686 (2009).
10. Haine, T. W. N. et al. Arctic freshwater export: status, mechanisms, and prospects. *Glob. Planet. Change* **125**, 13–35 (2015).
11. Hugelius, G. et al. Estimated stocks of circumpolar permafrost carbon with quantified uncertainty ranges and identified data gaps. *Biogeosciences* **11**, 6573–6593 (2014).
12. Gordeev, V. V. Fluvial sediment flux to the Arctic Ocean. *Geomorphology* **80**, 94–104 (2006).
13. Rawlins, M. A. et al. Analysis of the Arctic system for freshwater cycle intensification: observations and expectations. *J. Clim.* **23**, 5715–5737 (2010).
14. Whitefield, J., Winsor, P., McClelland, J. & Menemenlis, D. A new river discharge and river temperature climatology data set for the pan-Arctic region. *Ocean. Model.* **88**, 1–15 (2015).
15. McClelland, J. W. et al. Particulate organic carbon and nitrogen export from major Arctic rivers. *Glob. Biogeochem. Cycles* **30**, 1145–1165 (2016). **This paper presents POC and nitrogen fluxes for the Yukon, Mackenzie, Ob, Yenisei, Lena and Kolyma deltas from 9 years of field campaigns covering different seasons.**
16. Raymond, P. A. et al. Flux and age of dissolved organic carbon exported to the Arctic Ocean: a carbon isotopic study of the five largest Arctic rivers. *Glob. Biogeochem. Cycles* **21**, 1–9 (2007).
17. Obu, J. et al. Northern Hemisphere permafrost map based on TTOP modelling for 2000–2016 at 1 km² scale. *Earth Sci. Rev.* **193**, 299–316 (2019).
18. Bianchi, T. S. & Allison, M. A. Large-river delta-front estuaries as natural "recorders" of global environmental change. *Proc. Natl Acad. Sci. USA* **106**, 8085–8092 (2009).
19. Shields, M. R. et al. Carbon storage in the Mississippi River delta enhanced by environmental engineering. *Nat. Geosci.* **10**, 846–851 (2017).
20. Smith, R. W., Bianchi, T. S., Allison, M., Savage, C. & Galy, V. High rates of organic carbon burial in fjord sediments globally. *Nat. Geosci.* **8**, 450–453 (2015).
21. Olefeldt, D. et al. Circumpolar distribution and carbon storage of thermokarst landscapes. *Nat. Commun.* **7**, 13043 (2016).
22. Parmentier, F. J. W. et al. A synthesis of the Arctic terrestrial and marine carbon cycles under pressure from a dwindling cryosphere. *Ambio* **46**, 53–69 (2017).
23. Schuur, E. A. G. et al. Climate change and the permafrost carbon feedback. *Nature* **520**, 171–179 (2015).
24. Vonk, J. E. et al. Spatial variations in geochemical characteristics of the modern Mackenzie Delta sedimentary system. *Geochim. Cosmochim. Acta* **171**, 100–120 (2015).
25. Fuchs, M. et al. Sedimentary and geochemical characteristics of two small permafrost-dominated Arctic river deltas in northern Alaska. *Arktos* **4**, 1–18 (2018).
26. Schirrmeister, L. et al. Sedimentary characteristics and origin of the Late Pleistocene Ice Complex on north-east Siberian Arctic coastal lowlands and islands — a review. *Quat. Int.* **241**, 3–25 (2011).
27. Strauss, J. et al. Deep Yedoma permafrost: a synthesis of depositional characteristics and carbon vulnerability. *Earth Sci. Rev.* **172**, 75–86 (2017).
28. Bartlett, K. B., Crill, P. M., Sass, R. L., Harriss, R. C. & Dise, N. B. Methane emissions from tundra environments Yukon–Kuskokwim Delta, Alaska. *J. Geophys. Res.* **97**, 16,645–16,660 (1992).
29. Kohnert, K., Serafimovich, A., Metzger, S., Hartmann, J. & Sachs, T. Strong geologic methane emissions from discontinuous terrestrial permafrost in the Mackenzie Delta, Canada. *Sci. Rep.* **7**, 3–8 (2017).
30. Holmes, R. M. et al. A circumpolar perspective on fluvial sediment flux to the Arctic Ocean. *Glob. Biogeochem. Cycles* **16**, 1–14 (2002). **This is a comprehensive synthesis of observational data on fluvial sediment fluxes for the Yenisei, Lena, Ob, Mackenzie, Yukon, Pechora, Kolyma and Severnaya Dvina rivers, illustrating their relatively low sediment loads compared to rivers in lower latitudes**.
31. Piliouras, A., Lauzon, R. & Rowland, J. C. Unraveling the combined effects of ice and permafrost on Arctic delta morphodynamics. *J. Geophys. Res. Earth Surf.* **126**, 1–17 (2021).
32. Leffingwell, E. K. The Canning River region, northern Alaska. *USGS Prof. Pap.* **109**, 1–251 (1919).
33. Scott, K. M. Effects of permafrost on stream channel behavior in Arctic Alaska. *USGS Prof. Pap.* **1068**, 1–19 (1978).
34. Costard, F., Dupeyrat, L., Gautier, E. & Carey-Gailhardis, E. Fluvial thermal erosion investigations along a rapidly eroding river bank: application to the Lena River (central Siberia). *Earth Surf. Process. Landf.* **28**, 1349–1359 (2003). **This paper presents theoretical model development and field data of bank erosion in permafrost-affected rivers**.
35. Costard, F. et al. Impact of the global warming on the fluvial thermal erosion over the Lena River in central Siberia. *Geophys. Res. Lett.* **34**, 1–4 (2007).
36. Walker, J., Arnborg, L. & Peippo, J. Riverbank erosion in the Colville Delta. *Alaska. Geogr. Ann.* **69**, 61–70 (1987). **This paper presents observational data on slow rates of river bank erosion in different substrates and main versus distributary delta channels**.

37. Lauzon, R., Piliouras, A. & Rowland, J. C. Ice and permafrost effects on delta morphology and channel dynamics. *Geophys. Res. Lett.* **46**, 6574–6582 (2019).
This numerical modelling study investigates the effects of bank erodability on Arctic delta network topology.
38. Lim, Y. J., Levy, J. S., Goudge, T. A. & Kim, W. Ice cover as a control on the morphodynamics and stratigraphy of Arctic deltas. *Geology* **47**, 399–402 (2019).
39. *Snow, Water, Ice and Permafrost in the Arctic (SWIPA) 2017* (AMAP, 2017); https://www.amap.no/documents/download/2987/inline.
40. Hanna, E. et al. Greenland surface air temperature changes from 1981 to 2019 and implications for ice-sheet melt and mass-balance change. *Int. J. Climatol.* **41**, 1336–1352 (2020).
41. Turetsky, M. R. Permafrost collapse is accelerating carbon release. *Nature* **569**, 32–34 (2019).
42. Walvoord, M. A. & Kurylyk, B. L. Hydrologic impacts of thawing permafrost — a review. *Vadose Zone J.* **15**, 1–20 (2016).
43. Overeem, I. et al. Sea ice loss enhances wave action at the Arctic coast. *Geophys. Res. Lett.* **38**, L17503 (2011).
44. Barnhart, K. R., Overeem, I. & Anderson, R. S. The effect of changing sea ice on the physical vulnerability of Arctic coasts. *Cryosphere* **8**, 1777–1799 (2014).
The mapping of the onset of open water and its duration along the entire Arctic coast from remote-sensing data shows a 1.5–3-fold expansion of sea-ice-free conditions over the past three decades.
45. Hill, P. R., Blasco, S., Harper, J. & Fissel, D. Sedimentation on the canadian beaufort shelf. *Continental Shelf Res.* **11**, 821–842 (1991).
46. Hill, P. R., Peter Lewis, C., Desmarais, S., Kauppaymuthoo, V. & Rais, H. The Mackenzie Delta: sedimentary processes and facies of a high-latitude, fine-grained delta. *Sedimentology* **48**, 1047–1078 (2001).
47. Naidu, A. S. & Mowatt, T. C. in *Deltas: Models for Exploration* (ed. Broussard, M. L.) 283–309 (Houston Geological Society, 1975).
48. Dupre, W. R. & Thompson, R. The Yukon delta: a model for deltaic sedimentation in an ice-dominated environment. *Proc. Annu. Offshore Technol. Conf.* **5**, 657–664 (1979).
This classic description of delta processes in the Arctic setting was the first to propose using ice dominance as a classification criterion for high-latitude deltas.
49. Arnborg, L. & Walker, J. Suspended load in the Colville River, Alaska, 1962. *Geogr. Ann.* **49**, 131–144 (1966).
50. Walker, H. J. in *Symposium on the Hydrology of Deltas* 209–219 (IAHS, 1970).
51. Walker, H. J. & Hudson, P. F. Hydrologic and geomorphic processes in the Colville River delta, Alaska. *Geomorphology* **56**, 291–303 (2003).
52. Dupre, W. *Yukon Delta Coastal Processes Study* (OSTI, 1980); https://www.osti.gov/biblio/5793121-yukon-delta-coastal-processes-study-final-report.
53. Nelson, C. H., Dupre, W., Fleld, M. & Howard, J. D. Variations in sand body types on the Eastern Bering Sea epicontinental shelf. *Geol. Mijnbouw* **61**, 37–48 (1982).
54. Are, F. & Reimnitz, E. An overview of the Lena River Delta setting: geology, tectonics, geomorphology, and hydrology. *J. Coast. Res.* **16**, 1083–1093 (2000).
This is a synthesis paper on the long-term evolution of the Lena Delta.
55. Reimnitz, E. Interactions of river discharge with sea ice in proximity of Arctic deltas: a review. *Polarforschung* **70**, 123–134 (2000).
56. Reimnitz, E. & Bruder, K. River discharge into an ice-covered ocean and related sediment dispersal, Beaufort Sea, coast of Alaska. *Geol. Soc. Am. Bull.* **83**, 861–866 (1972).
57. Piliouras, A. & Rowland, J. C. Arctic river delta morphologic variability and implications for riverine fluxes to the coast. *J. Geophys. Res. Earth Surf.* **125**, 1–20 (2020).
58. Kasper, J. L. & Weingartner, T. J. The spreading of a buoyant plume beneath a landfast ice cover. *J. Phys. Oceanogr.* **45**, 478–494 (2015).
This process modelling study uses the Regional Ocean Model System to highlight the effects of sub-ice discharge of river water onto sea ice.
59. Emmerton, C. A., Lesack, L. F. W. & Marsh, P. Lake abundance, potential water storage, and habitat distribution in the Mackenzie River Delta, western Canadian Arctic. *Water Resour. Res.* **43**, 1–14 (2007).
This is a field study of carbon and nutrient exchanges between river floodwater and thermokarst lakes in the Mackenzie Delta, demonstrating sediment settling in the floodplain and organic matter enrichment sourced from lakes and the floodplain.
60. Nienhuis, J. H. et al. Global-scale human impact on delta morphology has led to net land area gain. *Nature* **577**, 514–518 (2020).
61. Bendixen, M. et al. Delta progradation in Greenland driven by increasing glacial mass loss. *Nature* **550**, 101–104 (2017).
62. Overeem, I. et al. Substantial export of suspended sediment to the global oceans from glacial erosion in Greenland. *Nat. Geosci.* **10**, 859–863 (2017).
63. Dickinson, W. in *New Perspectives in Basin Analysis* (eds Kleinspehn, K. & Paola, C.) 177–187 (Springer, 2011).
64. Spencer, A. M., Embry, A. F., Gautier, D. L., Stoupakova, A. V. & Sørensen, K. Chapter 1 An overview of the petroleum geology of the Arctic. *Geol. Soc. Lond. Mem.* **35**, 1–15 (2011).
65. Dick, H. J. B., Lin, J. & Schouten, H. An ultraslow-spreading class of ocean ridge. *Nature* **426**, 405–412 (2003).
66. Korotayev, V. N. Geomorphology of river deltas on the Arctic coast of Siberia. *Polar Geogr. Geol.* **10**, 139–147 (1986).
67. Schwamborn, G., Rachold, V. & Grigoriev, M. N. Late Quaternary sedimentation history of the Lena Delta. *Quat. Int.* **89**, 119–134 (2002).
68. Lane, L. S. Canada Basin, Arctic Ocean: evidence against a rotational origin. *Tectonics* **16**, 363–387 (1997).
69. Whitehouse, P. L., Allen, M. B. & Milne, G. A. Glacial isostatic adjustment as a control on coastal processes: an example from the Siberian Arctic. *Geology* **35**, 747–750 (2007).
This is a modelling study of glacio-isostatic rebound of Siberian deltas, demonstrating the effect of forebulge collapse on delta evolution.
70. Batchelor, C. L. et al. The configuration of Northern Hemisphere ice sheets through the Quaternary. *Nat. Commun.* **10**, 3713 (2019).
71. Klemann, V., Heim, B., Bauch, H. A., Wetterich, S. & Opel, T. Sea-level evolution of the Laptev Sea and the East Siberian Sea since the Last Glacial Maximum. *Arktos* **1**, 1–8 (2015).
72. Aarseth, I. Western Norwegian fjord sediments: age, volume, stratigraphy, and role as temporary depository during glacial cycles. *Mar. Geol.* **143**, 39–53 (1997).
73. Bolshiyanov, D., Makarov, A. & Savelieva, L. Lena River delta formation during the Holocene. *Biogeosciences* **12**, 579–593 (2015).
74. Peltier, W., Argus, D. & Drummond, R. Space geodesy constrains ice age terminal deglaciation: the global ICE-6G_C (VM5a) model. *J. Geophys. Res. Solid. Earth* **120**, 450–487 (2014).
75. Baranskaya, A. V. et al. A postglacial relative sea-level database for the Russian Arctic coast. *Quat. Sci. Rev.* **199**, 188–205 (2018).
76. Storms, J. E. A., de Winter, I. L., Overeem, I., Drijkoningen, G. G. & Lykke-Andersen, H. The Holocene sedimentary history of the Kangerlussuaq Fjord-valley fill, West Greenland. *Quat. Sci. Rev.* **35**, 29–50 (2012).
77. Overeem, I. & Syvitski, J. P. M. Experimental exploration of the stratigraphy of fjords fed by glaciofluvial systems. *Geol. Soc. Lond. Spec. Publ.* **344**, 125–142 (2010).
78. Fraser, C., Hill, P. R. & Allard, M. Morphology and facies architecture of a falling sea level strandplain, Umiujaq, Hudson Bay, Canada. *Sedimentology* **52**, 141–160 (2005).
79. O'Regan, M. et al. Early Holocene sea level in the Canadian Beaufort Sea constrained by radiocarbon dates from a deep borehole in the Mackenzie Trough, Arctic Canada. *Boreas* **47**, 1102–1117 (2018).
80. Hanna, A. J. M., Allison, M. A., Bianchi, T. S., Marcantonio, F. & Goff, J. A. Late Holocene sedimentation in a high Arctic coastal setting: Simpson Lagoon and Colville Delta, Alaska. *Cont. Shelf Res.* **74**, 11–24 (2014).
81. Peltier, W. R. Global glacial isostasy and the surface of the ice-age Earth: the ICE-5G (VM2) model and GRACE. *Annu. Rev. Earth Planet. Sci.* **32**, 111–149 (2004).
82. Clark, J. A., Farrell, W. E. & Peltier, W. R. Global changes in postglacial sea level: a numerical calculation. *Quat. Res.* **9**, 265–287 (1978).
83. National Oceanic and Atmospheric Administration. Sea level trends. *NOAA* https://tidesandcurrents.noaa.gov/sltrends/ (2021).
84. Love, R. et al. The contribution of glacial isostatic adjustment to projections of sea level change along the Atlantic and Gulf coasts of North America. *Earth's Future* **4**, 440–464 (2016).
85. Larour, E., Ivins, E. R. & Adhikari, S. Should coastal planners have concern over where land ice is melting? *Sci. Adv.* **3**, e1700537 (2017).
86. Galloway, W. E. in *Deltas, Models For Exploration* (ed. Broussard, M. L.) 87–98 (Houston Geological Society, 1975).
87. Syvitski, J. P. M. & Saito, Y. Morphodynamics of deltas under the influence of humans. *Glob. Planet. Change* **57**, 261–282 (2007).
88. Geleynse, N. et al. Controls on river delta formation; insights from numerical modelling. *Earth Planet. Sci. Lett.* **302**, 217–226 (2011).
89. Orton, G. & Reading, H. Variability of deltaic processes in terms of sediment supply, with particular emphasis on grain size. *Sedimentology* **40**, 475–512 (1993).
90. Edmonds, D. A. & Slingerland, R. L. Significant effect of sediment cohesion on delta morphology. *Nat. Geosci.* **3**, 105–109 (2010).
91. Caldwell, R. L. & Edmonds, D. A. The effects of sediment properties on deltaic processes and morphologies: a numerical modeling study. *J. Geophys. Res. Earth Surf.* **119**, 961–982 (2014).
92. Shaw, J. B., Mohrig, D. & Whitman, S. K. The morphology and evolution of channels on the Wax Lake delta, Louisiana, USA. *J. Geophys. Res. Earth Surf.* **118**, 1562–1584 (2013).
93. Wright, L. D. & Coleman, J. M. Mississippi River mouth processes: effluent dynamics and morphologic development. *J. Geol.* **82**, 751–778 (1974).
94. Overeem, I. et al. Small-scale stratigraphy in a large ramp delta: recent and Holocene sedimentation in the Volga Delta, Caspian Sea. *Sediment. Geol.* **159**, 133–157 (2003).
95. Coleman, J. M., Roberts, H. H. & Stone, G. W. Mississippi River delta: an overview. *J. Coast. Res.* **14**, 698–716 (1998).
96. Fagherazzi, S. Self-organization of tidal deltas. *Proc. Natl Acad. Sci. USA* **105**, 18692–18695 (2008).
97. Bhattacharya, J. P. in *Facies Models Revisited* (eds Posamentier, H. & Walker, R.) 237–292 (Society for Sedimentary Geology, 2006).
98. Hoitink, A. J. F., Wang, Z. B., Vermeulen, B., Huismans, Y. & Kästner, K. Tidal controls on river delta morphology. *Nat. Geosci.* **10**, 637–645 (2017).
99. Sassi, M. G., Hoitink, A. J. F., De Brye, B. & Deleersnijder, E. Downstream hydraulic geometry of a tidally influenced river delta. *J. Geophys. Res. Earth Surf.* **117**, 1–13 (2012).
100. Passalacqua, P., Lanzoni, S., Paola, C. & Rinaldo, A. Geomorphic signatures of deltaic processes and vegetation: the Ganges-Brahmaputra-Jamuna case study. *J. Geophys. Res. Earth Surf.* **118**, 1838–1849 (2013).
101. Bhattacharya, J. P. & Giosan, L. Wave-influenced deltas: geomorphological implications for facies reconstruction. *Sedimentology* **50**, 187–210 (2003).
102. Rodriguez, A. B., Hamilton, M. D. & Anderson, J. B. Facies and evolution of the modern Brazos Delta, Texas: wave versus flood influence. *J. Sediment. Res.* **70**, 283–295 (2000).
103. Nienhuis, J. H., Ashton, A. D. & Giosan, L. What makes a delta wave-dominated? *Geology* **43**, 511–514 (2015).
104. Wright, L. D. & Coleman, J. M. Variations in morphology of major river deltas as functions of ocean wave and river discharge regimes. *Am. Assoc. Pet. Geol. Bull.* **57**, 370–398 (1973).
105. Nienhuis, J. H., Ashton, A. D. & Giosan, L. Littoral steering of deltaic channels. *Earth Planet. Sci. Lett.* **453**, 204–214 (2016).
106. Wilson, C. A. & Goodbred, S. L. Jr Construction and maintenance of the Ganges-Brahmaputra-Meghna Delta: linking process, morphology, and stratigraphy. *Ann. Rev. Mar. Sci.* **7**, 67–88 (2015).
107. Solomon, S. M. Spatial and temporal variability of shoreline change in the Beaufort-Mackenzie region, northwest territories, Canada. *Geo-Marine Lett.* **25**, 127–137 (2005).
108. Syvitski, J. P. M. & Kettner, A. Sediment flux and the Anthropocene. *Phil. Trans. R. Soc. A* **369**, 957–975 (2011).

109. Egbert, G. D. & Erofeeva, S. Y. Efficient inverse modeling of barotropic ocean tides. *J. Atmos. Ocean. Technol.* **19**, 183–204 (2002).
110. Cancet, M., Andersen, O. B., Lyard, F., Cotton, D. & Benveniste, J. Arctide2017, a high-resolution regional tidal model in the Arctic Ocean. *Adv. Space Res.* **62**, 1324–1343 (2018).
111. Kulikov, M. E., Medvedev, I. P. & Kondrin, A. T. Features of seasonal variability of tidal sea-level oscillations in the Russian Arctic seas. *Russ. Meteorol. Hydrol.* **45**, 411–421 (2020).
112. Osadchiev, A. et al. Influence of estuarine tidal mixing on structure and spatial scales of large river plumes. *Ocean Sci.* **16**, 781–798 (2020).
113. Magritsky, D., Mikhailov, V., Korotaev, V. & Babich, D. Changes in hydrological regime and morphology of river deltas in the Russian Arctic. *IAHS-AISH Proc. Rep.* **358**, 67–79 (2013).
This is one of very few studies of sediment distribution and trapping within Arctic delta distributary networks.
114. *The GEBCO_2020 grid — a continuous terrain model of the global oceans and land* (NOC, 2020); https://www.bodc.ac.uk/data/published_data_library/catalogue/10.5285/a29c5465-b138-234d-e053-6c86abc040b9/.
115. Overeem, I. & Syvitski, J. P. M. Shifting discharge peaks in Arctic rivers, 1977–2007. *Geogr. Ann. Ser. A* **92**, 285–296 (2010).
116. Beltaos, S. Onset of river ice breakup. *Cold Reg. Sci. Technol.* **25**, 183–196 (1997).
117. Beltaos, S. Threshold between mechanical and thermal breakup of river ice cover. *Cold Reg. Sci. Technol.* **37**, 1–13 (2003).
118. Cooley, S. W. & Pavelsky, T. M. Spatial and temporal patterns in Arctic river ice breakup revealed by automated ice detection from MODIS imagery. *Remote Sens. Environ.* **175**, 310–322 (2016).
119. Yang, X., Pavelsky, T. M. & Allen, G. H. The past and future of global river ice. *Nature* **577**, 69–73 (2020).
120. Arp, C. D., Jones, B. J., Liljedahl, A. K., Hinkel, K. & Welker, J. Depth, ice thickness, and ice-out timing cause divergent hydrologic responses among Arctic lakes. *Water Resour. Res.* **51**, 9379–9401 (2015).
121. Jeffries, M. O., Morris, K. & Liston, G. E. A method to determine lake depth and water availability on the North Slope of Alaska with spaceborne imaging radar and numerical ice growth modelling. *Arctic* **49**, 367–374 (1996).
122. Goulding, H., Prowse, T. & Beltaos, S. Spatial and temporal patterns of break-up and ice-jam flooding in the Mackenzie Delta, NWT. *Hydrol. Process.* **23**, 2654–2670 (2009).
123. Vulis, L. et al. Channel network control on seasonal lake area dynamics in Arctic deltas. *Geophys. Res. Lett.* **47**, e2019GL086710 (2020).
124. Dean, K. G., Stringer, W. J., Ahlnas, K., Searcy, C. & Weingartner, T. The influence of river discharge on the thawing of sea ice, Mackenzie River delta: albedo and temperature analyses. *Polar Res.* **13**, 83–94 (1994).
125. Alkire, M. B. & Trefry, J. H. Transport of spring floodwater from rivers under ice to the Alaskan Beaufort Sea. *J. Geophys. Res. Ocean.* **111**, 1–12 (2006).
126. Wessells, S., Reimnitz, E., Barnes, P. & Kempema, E. Drift ice as a geologic agent (USGS, 1993).
An important USGS documentary film on field observations and laboratory experiments on ice–sediment transport and interactions.
127. Bareiss, J., Eicken, H., Helbig, A. & Martin, T. Impact of river discharge and regional climatology on the decay of sea ice in the laptev sea during spring and early summer. *Arct. Antarct. Alp. Res.* **31**, 214–229 (1999).
128. Nghiem, S., Hall, D. K., Rigor, I., Li, P. & Neumann, G. Effects of Mackenzie River discharge and bathymetry on sea ice in the Beaufort Sea. *Geophys. Res. Lett.* **41**, 873–879 (2014).
129. Barnhart, K. R. et al. Modeling erosion of ice-rich permafrost bluffs along the Alaskan Beaufort Sea coast. *J. Geophys. Res. Earth Surf.* **119**, 1155–1179 (2014).
130. Ravens, T. M., Jones, B. M., Zhang, J., Arp, C. D. & Schmutz, J. A. Process-based coastal erosion modeling for Drew Point, North Slope, Alaska. *J. Waterw. Port Coastal Ocean Eng.* **138**, 122–130 (2012).
131. Stettner, S. et al. Monitoring inter- and intra-seasonal dynamics of rapidly degrading ice-rich permafrost riverbanks in the Lena Delta with TerraSAR-X time series. *Remote Sens.* **10**, 51 (2018).
132. Hošeková, L. et al. Attenuation of ocean surface waves in pancake and frazil sea ice along the coast of the Chukchi Sea. *J. Geophys. Res. Ocean.* **125**, e2020JC016746 (2020).
133. Chikita, K. A. et al. in *Origin and Evolution of Natural Diversity International Symposium Proceedings* (HUSCAP, 2009).
134. Robert, A. & Tran, T. Mean and turbulent flow fields in a simulated ice-covered channel with a gravel bed: some laboratory observations. *Earth Surf. Process. Landf.* **37**, 951–956 (2012).
135. Lotsari, E. et al. Sub-arctic river bank dynamics and driving processes during the open-channel flow period. *Earth Surf. Process. Landf.* **45**, 1198–1216 (2020).
136. Sui, J., Wang, J., He, Y. & Krol, F. Velocity profiles and incipient motion of frazil particles under ice cover. *Int. J. Sediment. Res.* **25**, 39–51 (2010).
137. Lamb, E. & Toniolo, H. Initial quantification of suspended sediment loads for three Alaska North Slope rivers. *Water* **8**, 1–11 (2016).
138. Toniolo, H. et al. Hydraulic characteristics and suspended sediment loads during spring breakup in several streams located on the National Petroleum Reserve in Alaska, USA. *Nat. Resour.* **04**, 220–228 (2013).
139. Plug, L. J. & West, J. J. Thaw lake expansion in a two-dimensional coupled model of heat transfer, thaw subsidence, and mass movement. *J. Geophys. Res. Earth Surf.* **114**, 1–18 (2009).
140. Grosse, G., Jones, B. & Arp, C. Thermokarst lakes, drainage, and drained basins. *Treat. Geomorphol.* **8**, 325–353 (2013).
This is a comprehensive review of thermokarst lake formation and evolution.
141. Emmerton, C. A., Lesack, L. F. W. & Vincent, W. F. Mackenzie River nutrient delivery to the Arctic Ocean and effects of the Mackenzie Delta during open water conditions. *Glob. Biogeochem. Cycles* **22**, 1–15 (2008).
142. Marsh, P. et al. in *17th International Northern Research Basins Symposium Workshop* (Northern Research Basins Symposium, 2009).
143. Lesack, L. F. W. & Marsh, P. Lengthening plus shortening of river-to-lake connection times in the Mackenzie River Delta respectively via two global change mechanisms along the arctic coast. *Geophys. Res. Lett.* **34**, 1–6 (2007).
144. Vulis, L., Tejedor, A., Zaliapin, I., Rowland, J. C. & Foufoula-Georgiou, E. Climate signatures on lake and wetland size distributions in Arctic deltas. *Geophys. Res. Lett.* **48**, e2021GL094437 (2021).
145. Normandin, C. et al. Quantification of surface water volume changes in the Mackenzie Delta using satellite multi-mission data. *Hydrol. Earth Syst. Sci.* **22**, 1543–1561 (2018).
146. Forbes, D. L., Craymer, M. R. & Whalen, D. J. R. Subsidence and inundation of a large Arctic permafrost delta. In *Canadian Quaternary Association Conference* (2015).
147. Emmerton, C. A., Lesack, L. F. W. & Vincent, W. F. Nutrient and organic matter patterns across the Mackenzie River, estuary and shelf during the seasonal recession of sea-ice. *J. Mar. Syst.* **74**, 741–755 (2008).
148. Cunada, C. L., Lesack, L. F. W. & Tank, S. E. Methane emission dynamics among CO_2-absorbing and thermokarst lakes of a great Arctic delta. *Biogeochemistry* **156**, 375–399 (2021).
149. Kempema, E. W. & Barnes, P. W. Anchor ice, seabed freezing, and sediment dynamics in shallow Arctic seas. *J. Geophys. Res.* **92**, 671–678 (1987).
150. Kempema, E. W., Reimnitz, E., Clayton, J. R. & Payne, J. R. Interactions of frazil and anchor ice with sedimentary particles in a flume. *Cold Reg. Sci. Technol.* **21**, 137–149 (1993).
151. Hilton, R. G. et al. Erosion of organic carbon in the Arctic as a geological carbon dioxide sink. *Nature* **524**, 84–87 (2015).
Data analysis of the source-to-sink carbon pathway and storage in the prodelta of the Mackenzie Delta, pointing to the importance of the submarine domain as a hotspot of carbon sequestration.
152. Rowland, J. & Stauffer, S. Classified channel masks of portions of 13 rivers across the Arctic and areas of floodplain erosion and accretion ranging from 1973 to 2016. *ESS-DIVE* https://doi.org/10.15485/1571525 (2019).
153. Debol'skaya, E. I. A mathematical model of channel deformations in permafrost zone rivers. *Water Resour.* **41**, 512–521 (2014).
154. Zheng, L., Overeem, I., Wang, K. & Clow, G. D. Changing Arctic river dynamics cause localized permafrost thaw. *J. Geophys. Res. Earth Surf.* **124**, 2324–2344 (2019).
155. Vesakoski, J. M. et al. Arctic Mackenzie Delta channel planform evolution during 1983–2013 utilising Landsat data and hydrological time series. *Hydrol. Process.* **31**, 3979–3995 (2017).
156. Payne, C., Panda, S. & Prakash, A. Remote sensing of river erosion on the Colville River, North Slope Alaska. *Remote Sens.* **10**, 397 (2018).
157. Lantuit, H. et al. The Arctic Coastal Dynamics Database: a new classification scheme and statistics on Arctic permafrost coastlines. *Estuaries Coasts* **35**, 383–400 (2012).
158. Fritz, M., Vonk, J. E. & Lantuit, H. Collapsing Arctic coastlines. *Nat. Clim. Chang.* **7**, 6–7 (2017).
159. Gibbs, A. E. & Richmond, B. M. National assessment of shoreline change — summary statistics for updated vector shorelines and associated shoreline change data for the north coast of Alaska. *USGS Open File Rep.* **2017–1107**, 1–21 (2017).
160. Wobus, C. et al. Thermal erosion of a permafrost coastline: improving process-based models using time-lapse photography. *Arct. Antarct. Alp. Res.* **43**, 474–484 (2011).
161. Jones, B. M. et al. Increase in the rate and uniformity of coastline erosion in Arctic Alaska. *Geophys. Res. Lett.* **36**, 1–5 (2009).
162. Ping, C. L. et al. Soil carbon and material fluxes across the eroding Alaska Beaufort Sea coastline. *J. Geophys. Res. Biogeosci.* **116**, 1–12 (2011).
163. Fuchs, M. et al. Rapid fluvio-thermal erosion of a yedoma permafrost cliff in the Lena River delta. *Front. Earth Sci.* **8**, 1–18 (2020).
164. Jenner, K. A. & Hill, P. R. Recent, Arctic deltaic sedimentation: Olivier Islands, Mackenzie Delta, North-west Territories, Canada. *Sedimentology* **45**, 987–1004 (1998).
165. Cohen, S., Kettner, A. J., Syvitski, J. P. M. & Fekete, B. M. WBMsed, a distributed global-scale riverine sediment flux model: model description and validation. *Comput. Geosci.* **53**, 80–93 (2013).
166. Chawla, A., Spindler, D. M. & Tolman, H. L. Validation of a thirty year wave hindcast using the Climate Forecast System Reanalysis winds. *Ocean Model.* **70**, 189–206 (2013).
167. Jerolmack, D. J. & Swenson, J. B. Scaling relationships and evolution of distributary networks on wave-influenced deltas. *Geophys. Res. Lett.* **34**, 1–5 (2007).
168. Patruno, S. & Helland-Hansen, W. Clinoforms and clinoform systems: review and dynamic classification scheme for shorelines, subaqueous deltas, shelf edges and continental margins. *Earth Sci. Rev.* **185**, 202–233 (2018).
169. Donchyts, G. et al. Earth's surface water change over the past 30 years. *Nat. Clim. Chang.* **6**, 810–813 (2016).
170. Fyfe, J. C. et al. One hundred years of Arctic surface temperature variation due to anthropogenic influence. *Sci. Rep.* **3**, 1–7 (2013).
171. Moon, T. A. et al. The expanding footprint of rapid Arctic change. *Earth's Future* **7**, 212–218 (2019).
172. Jorgenson, M. T., Shur, Y. L. & Pullman, E. R. Abrupt increase in permafrost degradation in Arctic Alaska. *Geophys. Res. Lett.* **33**, 2–5 (2006).
173. Bring, A. et al. Arctic terrestrial hydrology: a synthesis of processes, regional effects, and research challenges. *J. Geophys. Res. G* **121**, 621–649 (2016).
174. Burn, C. R. & Kokelj, S. V. The environment and permafrost of the Mackenzie Delta area. *Permafr. Periglac. Process.* **20**, 83–105 (2009).
175. Arp, C. D., Jones, B. M., Schmutz, J. A., Urban, F. E. & Jorgenson, M. T. Two mechanisms of aquatic and terrestrial habitat change along an Alaskan Arctic coastline. *Polar Biol.* **33**, 1629–1640 (2010).
176. Herman-Mercer, N., Schuster, P. & Maracle, K. Indigenous observations of climate change in the Lower Yukon River Basin, Alaska. *Hum. Organ.* **70**, 244–252 (2011).
177. Peterson, B. J. et al. Increasing river discharge to the Arctic Ocean. *Science.* **298**, 2171–2173 (2002).
178. Dankers, R. & Middelkoop, H. River discharge and freshwater runoff to the Barents Sea under present and future climate conditions. *Clim. Change* **87**, 131–153 (2008).
179. Vernon, C. L. et al. Surface mass balance model intercomparison for the Greenland ice sheet. *Cryosphere* **7**, 599–614 (2013).
180. Box, J. E. et al. Global sea-level contribution from Arctic land ice: 1971–2017. *Environ. Res. Lett.* **13**, 125012 (2018).

181. National Snow & Ice Data Center. Charctic interactive sea ice graph. *NSIDC* https://nsidc.org/arcticseaicenews/charctic-interactive-sea-ice-graph/ (2020).
182. Stopa, J. E., Ardhuin, F. & Girard-Ardhuin, F. Wave climate in the Arctic 1992–2014: seasonality and trends. *Cryosphere* **10**, 1605–1629 (2016).
183. Waseda, T. et al. Correlated increase of high ocean waves and winds in the ice-free waters of the Arctic Ocean. *Sci. Rep.* **8**, 4489 (2018).
184. Davy, R. & Outten, S. The Arctic surface climate in CMIP6: status and developments since CMIP5. *J. Clim.* **33**, 8047–8068 (2020).
185. Syvitski, J. P. M. Sediment discharge variability in Arctic rivers: implications for a warmer future. *Polar Res.* **21**, 323–330 (2002).
186. Dunn, F. E. et al. Projections of declining fluvial sediment delivery to major deltas worldwide in response to climate change and anthropogenic stress. *Environ. Res. Lett.* **14**, 084034 (2019).
187. Barnhart, K. R., Miller, C. R., Overeem, I. & Kay, J. E. Mapping the future expansion of Arctic open water. *Nat. Clim. Chang.* **6**, 280–285 (2015).
188. Casas-Prat, M. & Wang, X. L. Projections of extreme ocean waves in the Arctic and potential implications for coastal inundation and erosion. *J. Geophys. Res. Oceans* **125**, e2019JC015745 (2020).
This paper presents projections of future Arctic Ocean wave conditions using the well established WaveWatch III model, which shows a threefold increase in wave energy over the twenty-first century.
189. Antonova, S. et al. Thaw subsidence of a yedoma landscape in Northern Siberia, measured in situ and estimated from TerraSAR-X Interferometry. *Remote Sens.* **10**, 494 (2018).
190. O'Neill, B., Smith, S. L. & Duchesne, C. in *18th International Conference on Cold Regions Engineering and 8th Canadian Permafrost Conference* (American Society of Civil Engineers, 2019).
191. Jorgenson, T. M., Frost, G. V. & Dissing, D. Drivers of landscape changes in coastal ecosystems on the Yukon-Kuskokwim Delta, Alaska. *Remote Sens.* **10**, 1–27 (2018).
192. Elmendorf, S. C. et al. Plot-scale evidence of tundra vegetation change and links to recent summer warming. *Nat. Clim. Chang.* **2**, 453–457 (2012).
193. Nitze, I. & Grosse, G. Detection of landscape dynamics in the Arctic Lena Delta with temporally dense Landsat time-series stacks. *Remote Sens. Environ.* **181**, 27–41 (2016).
194. Bjorkman, A. D. et al. Plant functional trait change across a warming tundra biome. *Nature* **562**, 57–62 (2018).
195. Macreadie, P. I. et al. The future of Blue Carbon science. *Nat. Commun.* **10**, 3998 (2019).
196. Lasserre, F. Simulations of shipping along Arctic routes: comparison, analysis and economic perspectives. *Polar Rec.* **51**, 239–259 (2015).
197. Eguíluz, V. M., Fernández-Gracia, J., Irigoien, X. & Duarte, C. M. A quantitative assessment of Arctic shipping in 2010–2014. *Sci. Rep.* **6**, 3–8 (2016).
198. Gulas, S., Downton, M., D'Souza, K., Hayden, K. & Walker, T. R. Declining Arctic Ocean oil and gas developments: opportunities to improve governance and environmental pollution control. *Mar. Policy* **75**, 53–61 (2017).
199. Bendixen, M. et al. Promises and perils of sand exploitation in Greenland. *Nat. Sustain.* **2**, 98–104 (2019).
200. Wenzel, G. W. Canadian Inuit subsistence and ecological instability — if the climate changes, must the Inuit? *Polar Res.* **28**, 89–99 (2009).
201. Zeller, D., Booth, S., Pakhomov, E., Swartz, W. & Pauly, D. Arctic fisheries catches in Russia, USA, and Canada: baselines for neglected ecosystems. *Polar Biol.* **34**, 955–973 (2011).
202. Pisaric, M. F. J. et al. Impacts of a recent storm surge on an Arctic delta ecosystem examined in the context of the last millennium. *Proc. Natl Acad. Sci. USA* **108**, 8960–8965 (2011).
203. Notz, D. Arctic sea ice in CMIP6. *Geophys. Res. Lett.* **47**, e2019GL086749 (2020).
204. Jafarov, E. E., Marchenko, S. S. & Romanovsky, V. E. Numerical modeling of permafrost dynamics in Alaska using a high spatial resolution dataset. *Cryosphere* **6**, 613–624 (2012).
205. McGuire, A. D. et al. Dependence of the evolution of carbon dynamics in the northern permafrost region on the trajectory of climate change. *Proc. Natl Acad. Sci. USA* **115**, 201719903 (2018).
206. Clow, G. D. CVPM 1.1: a flexible heat-transfer modeling system for permafrost. *Geosci. Model. Dev.* **11**, 4889–4908 (2018).
207. Overeem, I. et al. A modeling toolbox for permafrost landscapes. *Eos* https://doi.org/10.1029/2018EO105155 (2018).
208. Wang, K., Jafarov, E. & Overeem, I. Sensitivity evaluation of the Kudryavtsev permafrost model. *Sci. Total Environ.* **720**, 137538 (2020).
209. Matell, N. et al. Modeling the subsurface thermal impact of Arctic thaw lakes in a warming climate. *Comput. Geosci.* **53**, 69–79 (2013).
210. Dupeyrat, L. et al. Effects of ice content on the thermal erosion of permafrost: implications for coastal and fluvial erosion. *Permafr. Periglac. Process.* **22**, 179–187 (2011).
211. Kobayashi, N., Vidrine, J. C., Nairn, R. B. & Soloman, S. M. Erosion of frozen cliffs due to storm surge on Beaufort Sea coast. *J. Coast. Res.* **15**, 332–344 (1999).
212. Baar, A. W., Boechat Albernaz, M., van Dijk, W. M. & Kleinhans, M. G. Critical dependence of morphodynamic models of fluvial and tidal systems on empirical downslope sediment transport. *Nat. Commun.* **10**, 4903 (2019).
213. Shen, H. H. Modelling ocean waves in ice-covered seas. *Appl. Ocean Res.* **83**, 30–36 (2019).
214. Hülse, P. & Bentley, S. J. A 210Pb sediment budget and granulometric record of sediment fluxes in a subarctic deltaic system: the Great Whale River, Canada. *Estuar. Coast. Shelf Sci.* **109**, 41–52 (2012).
215. Rogers, W. E. Implementation of sea ice in the wave model SWAN (Naval Research Laboratory, 2019).
216. Lehner, B. & Grill, G. Global river hydrography and network routing: baseline data and new approaches to study the world's large river systems. *Hydrol. Process.* **27**, 2171–2186 (2013).
217. Amante, C. & Eakins, B. W. ETOPO1 1 Arc-Minute Global Relief Model: procedures, data sources and analysis (National Geophysical Data Center, 2009).
218. US Geological Survey. *USGS water data for the nation*. *USGS* https://waterdata.usgs.gov/nwis (2021).
219. Government of Canada. Historical hydrometric data. *GC* https://wateroffice.ec.gc.ca/mainmenu/historical_data_index_e.html (2021).
220. Carson, M. A., Jasper, J. N. & Conly, F. M. Magnitude and sources of sediment input to the Mackenzie Delta, Northwest Territories, 1974–94. *Arctic* **51**, 116–124 (1998).
221. Lesack, L. F. W., Marsh, P., Hicks, F. E. & Forbes, D. L. Breakup in a large Arctic delta. *Geophys. Res. Lett.* **41**, 1560–1566 (2014).
222. National Weather Service. River breakup database. *NOAA* https://www.weather.gov/aprfc/breakupDB?site=488 (2020).
223. Nienhuis, J. H. & van de Wal, R. S. W. Projections of global delta land loss from sea-level rise in the 21st century. *Geophys. Res. Lett.* **48**, 1–9 (2021).
224. Kroon, A. et al. Deltas, freshwater discharge, and waves along the Young Sound, NE Greenland. *Ambio* **46**, 132–145 (2017).
This paper investigates interacting process controls on several deltas in East Greenland, demonstrating the dominance of fluvial processes and the seasonality of wave-driven sediment transport.
225. Corner, G. D. in *Incised Valleys in Time and Space* Vol. 85 (eds Dalrymple, R. W., Leckie, D. A. & Tilan, R. W.) 161–178 (Society for Sedimentary Geology, 2006).
226. Hansen, L. Deltaic infill of a deglaciated arctic fjord, East Greenland: sedimentary facies and sequence stratigraphy. *J. Sediment. Res.* **74**, 422–437 (2004).
227. Bendixen, M. & Kroon, A. Conceptualizing delta forms and processes in Arctic coastal environments. *Earth Surf. Process. Landf.* **42**, 1227–1237 (2017).
228. Carrivick, J. L. & Quincey, D. J. Progressive increase in number and volume of ice-marginal lakes on the western margin of the Greenland Ice Sheet. *Glob. Planet. Change* **116**, 156–163 (2014).
229. North Slope Science Initiative. 2016 Colville River Delta spring breakup monitoring and hydrological assessment (NSSI, 2016).
230. How, P. et al. Greenland-wide inventory of ice marginal lakes using a multi-method approach. *Sci. Rep.* **11**, 4481 (2021).
231. Mernild, S. H. & Hasholt, B. Observed runoff, jokulhlaups and suspended sediment load from the Greenland ice sheet at Kangerlussuaq, West Greenland, 2007 and 2008. *J. Glaciol.* **55**, 855–858 (2009).
232. Mikkelsen, A. B., Hasholt, B., Knudsen, N. T. & Nielsen, M. H. Jokulhlaups and sediment transport in Watson River, Kangerlussuaq, West Greenland. *Hydrol. Res.* **44**, 58–67 (2013).
233. Russell, A. J., Carrivick, J. L., Ingeman-Nielsen, T., Yde, J. C. & Williams, M. A new cycle of jökulhlaups at Russell Glacier, Kangerlussuaq, West Greenland. *J. Glaciol.* **57**, 238–246 (2011).

Acknowledgements
The authors acknowledge funding from the US National Science Foundation (NSF-OPP awards 2001225 and 1844181).

Author contributions
The authors contributed equally to all aspects of the article.

Competing interests
The authors declare no competing interests.

Peer review information
Nature Reviews Earth & Environment thanks Y. Saito, A. Kroon and L. Vulis, who co-reviewed with E. Foufoula-Georgiou, for their contribution to the peer review of this work.

Publisher's note
Springer Nature remains neutral with regard to jurisdictional claims in published maps and institutional affiliations.

Supplementary information
The online version contains supplementary material available at https://doi.org/10.1038/s43017-022-00268-x.

RELATED LINKS
ArcticDEM: https://www.pgc.umn.edu/data/arcticdem/